





ORIGINAL ARTICLE

Neuroanatomy of the crocodylomorph *Portugalosuchus azenhae* from the late cretaceous of Portugal

Eduardo Puértolas-Pascual^{1,2,3}  | Ivan T. Kuzmin⁴  | Alejandro Serrano-Martínez⁵  | Octávio Mateus^{2,3} 

¹Aragosaurus-IUCA, Departamento de Ciencias de la Tierra, Facultad de Ciencias, Universidad de Zaragoza, Zaragoza, Spain

²GeoBioTec, Departamento de Ciências da Terra FCT, Universidade Nova de Lisboa, Caparica, Portugal

³Museu da Lourinhã, Lourinhã, Portugal

⁴Department of Vertebrate Zoology, Saint Petersburg State University, St. Petersburg, Russian Federation

⁵Institut Català de Paleontologia Miquel Crusafont, Universitat Autònoma de Barcelona, Barcelona, Spain

Correspondence

Eduardo Puértolas-Pascual, Aragosaurus reconstrucciones paleoambientales-IUCA, Departamento de Ciencias de la Tierra, Facultad de Ciencias, Universidad de Zaragoza. Calle Pedro Cerbuna 12, 50009, Zaragoza, Spain.
Email: puertolas@unizar.es

Funding information

Fundação para a Ciência e a Tecnologia (Government of Portugal), Grant/Award Number: GeoBioTec UIDB/04035/2020 and SFRH/BPD/116759/2016; Ministerio de Universidades (Government of Spain); EU Next Generation program (European Union), Grant/Award Number: Postdoctoral contract (María Zambrano); Ministerio de Ciencia e Innovación (Government of Spain), Grant/Award Number: PID2021-122612OB-I00

Abstract

We present the first detailed braincase anatomical description and neuroanatomical study of *Portugalosuchus azenhae*, from the Cenomanian (Late Cretaceous) of Portugal. This eusuchian crocodylomorph was originally described as a putative Crocodylia and one of the oldest representatives of this clade; however, its phylogenetic position remains controversial. Based on new data obtained from high resolution Computed Tomography images (by micro-CT scan), this study aims to improve the original description of this taxon and also update the scarce neuroanatomical knowledge of Eusuchia and Crocodylia from this time interval, a key period to understand the origin and evolution of these clades. The resulting three-dimensional models from the CT data allowed a detailed description of its well-preserved neurocranium and internal cavities. Therefore, it was possible to reconstruct the cavities of the olfactory region, nasopharyngeal ducts, brain, nerves, carotid arteries, blood vessels, paratympenic sinus system and inner ear, which allowed to estimate some neurosensorial capabilities. By comparison with other crocodylomorphs, these analyses showed that *Portugalosuchus*, back in the Cenomanian, already displayed an olfactive acuity, sight, hearing and cognitive skills within the range of that observed in other basal eusuchians and crocodylians, including extant species. In addition, and in order to test its disputed phylogenetic position, these new anatomical data, which helped to correct and complete some of the original observations, were included in one of the most recent morphology-based phylogenies. The position of *Portugalosuchus* differs slightly from the original publication since it is now located as a “thoracosaurid” within Gavialoidea, but still as a crocodylian. Despite all this, to better contrast these results, additional phylogenetic analyses including this new morphological character coding together with DNA data should be performed.

KEYWORDS

braincase, Cenomanian, Crocodylia, Eusuchia, neurosensorial capabilities, phylogeny

This is an open access article under the terms of the [Creative Commons Attribution-NonCommercial](https://creativecommons.org/licenses/by-nc/4.0/) License, which permits use, distribution and reproduction in any medium, provided the original work is properly cited and is not used for commercial purposes.

© 2023 The Authors. *Journal of Anatomy* published by John Wiley & Sons Ltd on behalf of Anatomical Society.

1 | INTRODUCTION

1.1 | Neuroanatomical studies on Crocodylomorpha

Since the first neuroanatomical studies on fossil crocodylomorphs by Owen (1842, 1850), advances in this discipline have not stopped growing, especially with the beginning of the 21st century. This increase in recent decades is due to the widespread use of Computerized Tomography (CT) to scan fossil and extant skulls, since, before this technology, these studies were based on natural and artificial endocasts and broken specimens (e.g., Serrano-Martínez, 2019 and references therein). The use of CT scan technology in paleontology allows the reconstruction of the internal structures and soft tissues that filled the inner cavities of the skulls (e.g., Witmer et al., 2008).

The first digital three-dimensional reconstructions of cranial cavities of extinct crocodylomorphs by using CT images were obtained from the notosuchians *Anatosuchus*, *Araripesuchus* (Serenó & Larsson, 2009) and *Simosuchus* (Kley et al., 2010). Regarding this clade, neuroanatomical studies on notosuchian taxa remain scarce, although their relevance is increasing in recent years. For example, stand out the works on three-dimensional reconstructions of the cranial cavities of *Sebecus* (Colbert et al., 1946), *Wargosuchus* (Martinelli & Pais, 2008), *Zulmasuchus* (Pochat-Cottilloux et al., 2022), *Mariliasuchus* (Maria et al., 2010; Rodrigues et al., 2010), *Rukwasuchus* (Sertich & O'Connor, 2014), *Araripesuchus* (Fernández-Dumont et al., 2017), *Campinasuchus* (Fonseca et al., 2020) and *Baurusuchus* (Dumont Jr et al., 2022).

Neuroanatomical research on basalmost crocodylomorphs is relatively scarce. To date, only a few studies on the endocranial anatomy and paratympanic pneumaticity have been published: e.g., for the noncrocodyliform crocodylomorphs *Sphenosuchus* (Walker, 1990), *Macelognathus* (Leardi et al., 2017), and *Almadasuchus* (Leardi et al., 2020) and the basal crocodyliform *Eopneumatosuchus* (Melstrom et al., 2022).

Regarding other groups, Thalattosuchia is probably the extinct crocodylomorph clade that has produced more studies on its neuroanatomy. We can highlight several works on neurosensory analyses (Brusatte et al., 2016; Pierce et al., 2017) and palaeoecological and phylogenetical implications of their neuroanatomy (Herrera et al., 2018; Schwab et al., 2020). But the most abundant works are about descriptions of the inner skull cavities, including taxa such as *Cricosaurus* (Fernández & Gasparini, 2000, 2008; Fernández & Herrera, 2009; Herrera, 2015; Herrera et al., 2013, 2018), 'Metriorhynchus' (Fernández et al., 2011; Schwab et al., 2021), *Dakosaurus* (Herrera & Vennari, 2015), *Plagiophtalmosuchus* (Brusatte et al., 2016), *Macrospodylus* (Herrera et al., 2018; Wilberg et al., 2022), *Maledictosuchus* (Parrilla-Bel et al., 2016) and *Pelagosaurus* (Pierce et al., 2017).

Several studies have been published on the neuroanatomy of noneusuchian neosuchians: e.g., dyrosaurid *Rhabdognathus* (Erb & Turner, 2021), pholidosaurid *Pholidosaurus* and the putative

goniopholidid '*Goniopholis pugnax*' (Edinger, 1938). Among Eusuchia, most of the works are focused on the neuroanatomy of the crown-group Crocodylia. Thanks to CT scans, silicone casting, and cranial dissections, descriptive works of the inner skull cavities and soft tissue from extant crocodylians stand out (e.g., Bona et al., 2017; Brusatte et al., 2016; Colbert, 1946; Franzosa, 2004; Hopson, 1979; Kawabe et al., 2009; Kuzmin et al., 2021; Lessner, 2021; Lessner & Holliday, 2022; Owen, 1850; Pierce et al., 2017; Schwab et al., 2022; Serrano-Martínez, 2019; Tarsitano, 1985; Witmer et al., 2008; Witmer & Ridgely, 2009). In addition, several studies on the ontogeny of the skull cavities of extant crocodylians have also been carried out (Dufeu & Witmer, 2015; Hu et al., 2021; Jirak & Janacek, 2017; Kuzmin et al., 2021; Watanabe et al., 2019).

In contrast, neuroanatomical studies on fossil eusuchians remain scarce. On noncrocodylian basal eusuchians, there are a few papers about *Aegisuchus* (Holliday & Gardner, 2012) and Allodaposuchidae (Blanco et al., 2015; Puértolas-Pascual et al., 2022; Serrano-Martínez, 2019; Serrano-Martínez et al., 2019a, 2021). And, regarding fossil crocodylians, these kinds of studies are even scarcer, with just some papers about the basal alligatoroid *Diplocynodon* (Serrano-Martínez et al., 2019b) and derived caimanine alligatoroid *Mourasuchus* (Bona et al., 2013), the gavialoids *Thoracosaurus* (Lemoine, 1883) and *Gryposuchus* (Bona et al., 2017), the tomistomines *Maomingosuchus* ('Tomistoma') (Yeh, 1958) and *Gunggamarandu* (Ristevski et al., 2021), and the mekosuchines crocodyloid *Paludirex* and *Trilophosuchus* (Ristevski, 2022; Ristevski et al., 2020).

The oldest representatives of Eusuchia have a record since the Early Cretaceous of Europe (Clark & Norell, 1992) to be the dominant crocodylomorph clade during the Late Cretaceous and Cenozoic ecosystems of this continent (see Puértolas-Pascual et al., 2016 and references therein). The braincase studied here corresponds to the skull of *Portugalosuchus azenhae* Mateus et al. (2019), from the Late Cretaceous (Cenomanian) of Casais dos Carecos, Coimbra (Portugal). The specimen (ML1818) was recovered from marine mixed siliciclastic-carbonate deposits in the West Portuguese Carbonate Platform (Mateus et al., 2019). This eusuchian crocodylomorph was originally described as a putative Crocodylia, and may be the oldest representative of this clade (Mateus et al., 2019; Rio & Mannion, 2021). Therefore, the present study aims to update the scarce neuroanatomical knowledge of taxa from the early radiation of Eusuchia and the origin of the crown-group Crocodylia by studying the neuroanatomy and neurosensory capabilities of *Portugalosuchus*. Crocodylomorph remains from this time interval are scarce worldwide; therefore, this work may provide important information about the development of the brain structures in eusuchians and the first crocodylians. In addition, and thanks to the new anatomical information observed from the CT scan of this specimen, it has been possible to update the cladistic matrix (Supplementary Information S2) with new codification of several characters. This allowed us to perform a more accurate phylogenetic analysis that places *Portugalosuchus* as a "thoracosaurid" within the crown-group Crocodylia.

2 | MATERIALS AND METHODS

The specimen here studied corresponds to the skull (Figures 1 and 2) and mandible (Figure 3) holotype of *Portugalosuchus azenhae* (ML1818), which is housed in the collection of the Museu da Lourinhã (Lourinhã, Portugal). The specimen was almost completely prepared (some areas still have rock matrix) using a compressed air scribe hammer and consolidated with Paraloid B-72 before image acquisition.

To perform the three-dimensional reconstructions (Figures 2–6), the skull and mandible were analyzed by CT scan. ML1818 was scanned with the micro-CT (V|Tome|X s 240 of GE Sensing & Inspections Technologies) at the Centro Nacional de Investigación sobre Evolución Humana (CENIEH) (Burgos, Spain), with a voltage of 170kV (160kV for the mandible scan) and a current intensity of 250µA. The resulting scan yielded 1599 images (3048 for the mandible scan) with 0.11000033mm voxel size (0.05649985 for the mandible scan) and image resolution of 2024 × 2024 pixels. Raw data from the scan were imported, processed and segmented with the software Avizo Software 2020.3 (Thermo Fisher Scientific). The 3D models obtained were rendered with Blender v. 2.90.1 (Blender Foundation).

The terminology and color pattern of the figures are based on: Witmer et al. (2008) for the brain cavities; Holliday and Witmer (2009) and Lessner and Holliday (2022) for the nerves; and Dufeu and Witmer (2015) and Kuzmin et al. (2021) for the paratympanic sinus system and the inner ear.

The three-dimensional reconstruction of the inner cavities (Figures 7–10) and neurosensory analyses of ML1818 were compared with multiple available crocodylomorphs specimens digitally reconstructed († = extinct taxa). Among the crown-group Crocodylia, ML1818 was compared with the basal alligatoroid †*Diplocynodon tormis* Buscalioni et al. (1992) (STUS-344; Serrano-Martínez et al., 2019b), the alligatorines *Alligator mississippiensis* (Daudin, 1802) (OUVC-9761, Witmer & Ridgely, 2008; 13 specimens from Dufeu & Witmer, 2015; MZB 92-0231, Serrano-Martínez et al., 2019a; and DVZ M 4/13, Kuzmin et al., 2021) and *Alligator sinensis* Fauvel, 1879 (DVZ M 2/13 and 3/13, Kuzmin et al., 2021), and the caimanines *Caiman crocodilus* Linnaeus, 1758 (FMNH 73711, Brusatte et al., 2016; and caiman_crocodylus_CRARC, Serrano-Martínez et al., 2019a), *Caiman yacare* Daudin, 1802 (ZMMU MSU R-6967, Kuzmin et al., 2021), *Melanosuchus niger* (Spix, 1825) (RVC-JRH-FBC1, Serrano-Martínez et al., 2021) and †*Mourasuchus nativus* (Gasparini, 1985) (MLP 73-IV-15-9, Bona et al., 2013). Among

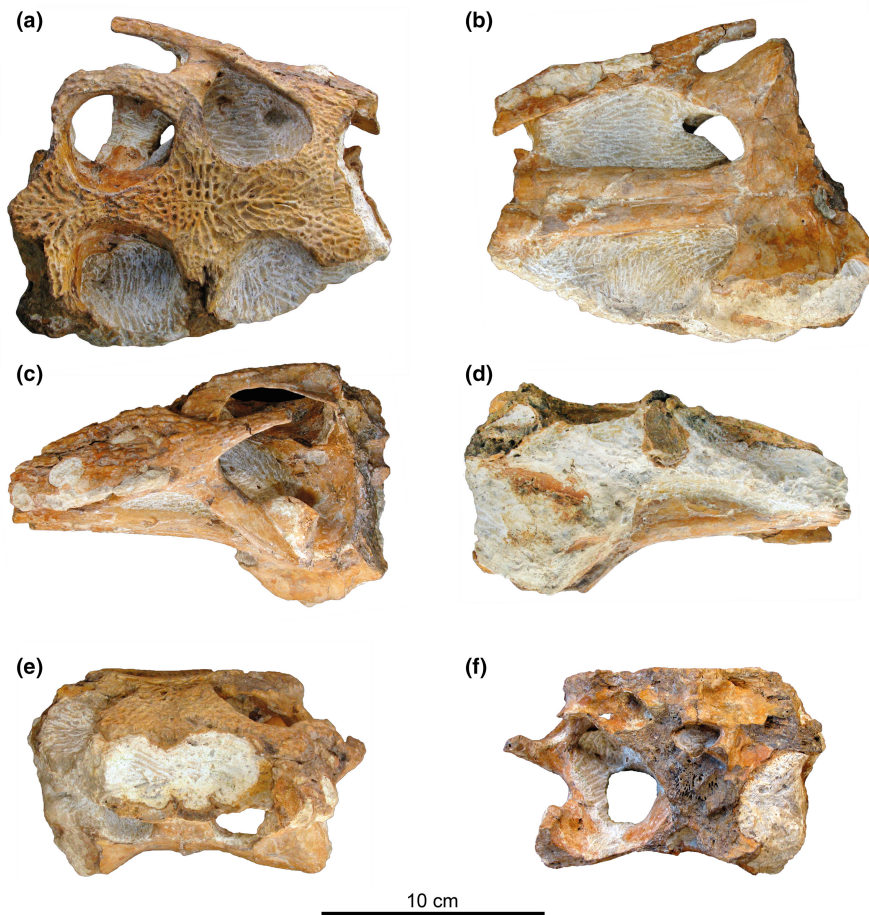


FIGURE 1 Photographs of the skull of the holotype of *Portugalosuchus azenhae* (ML1818) in: dorsal (a), ventral (b), left lateral (c), right lateral (d), anterior (e) and posterior (f) views.

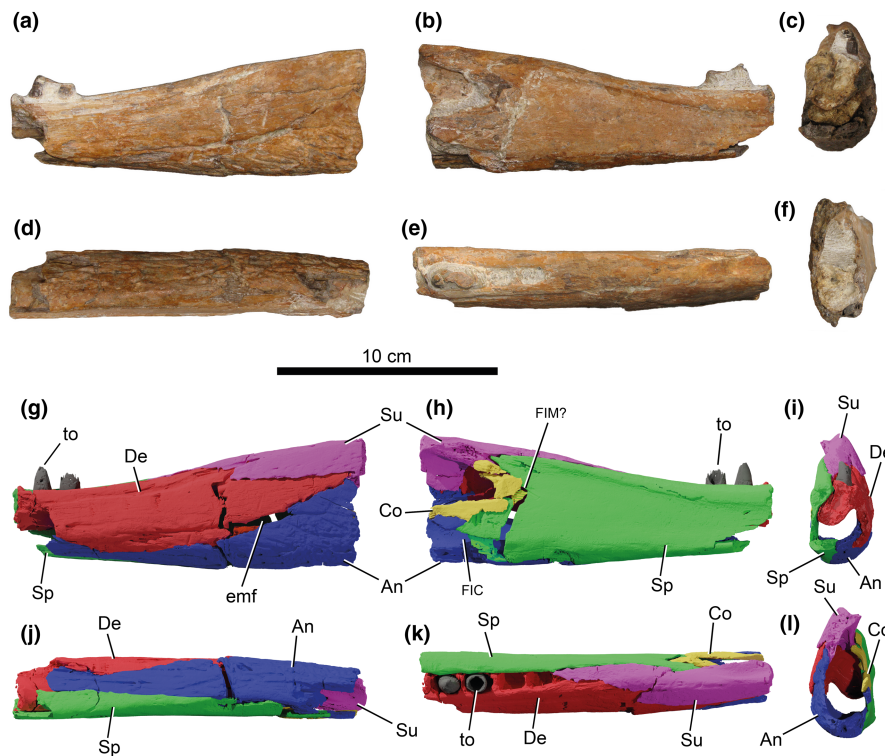


FIGURE 3 Photographs and three-dimensional reconstruction of the left mandible of the holotype of *Portugalosuchus azenhae* (ML1818) in: lateral (a, g), medial (b, h), anterior (c, i), ventral (d, j), dorsal (e, k) and posterior (f, l) views. For anatomical abbreviations, see Material and methods section.

PV OR 33095, Brusatte et al., 2016), †*Macrospondylus* (BSPG 1984 I258, Herrera et al., 2018; MCZ VPRA-1063, Wilberg et al., 2022), †*Cricosaurus* (MLP 72-IV-7-1, Herrera et al., 2018), †*Pelagosaurus* (BRLSI M1413; Pierce et al., 2017) and †*Metriorhynchus* (MDA 2; Fernández et al., 2011).

2.1 | Institutional abbreviations

BRLSI, Bath Royal Literary and Scientific Institute, Bath, UK; BSPG, Bayerische Staatssammlung für Paläontologie und Geologie, Munich, Germany; CCMGE, Chernyshev's Central Museum of Geological Exploration, Saint Petersburg, Russia; CENIEH, Centro Nacional de Investigación de La Evolución Humana, Burgos, Spain; CMC, Chinchilla Museum Collection, Chinchilla, Queensland, Australia; CRARC, Centre de Recuperació d'Amfibis i Rèptils de Catalunya, Barcelona, Spain; CPPLIP, Centro de Pesquisas Paleontológicas "Llewellyn Ivor Price" Universidade Federal do Triângulo Mineiro (UFTM), Peirópolis, Uberaba, Minas Gerais, Brazil; DVZ M, morphological collection of Department of Vertebrate Zoology of Saint Petersburg State University, Saint Petersburg, Russia; FMNH, Field Museum of Natural History, Chicago, Illinois, USA; IFSP-VTP, Instituto Federal de Educação, Ciência e Tecnologia São Paulo, Votuporanga, São Paulo, Brazil; IGM, Mongolian Institute of Geology, Ulaan Bataar, Mongolia; MCD, Museu de la Conca Dellà, Lleida, Spain; ML, Museu da Lourinhã; MDA, Museo del Desierto de Atacama, Antofagasta,

Chile; MLP, Museo de La Plata, Buenos Aires, Argentina; MPZ, Museo de Ciencias Naturales de la Universidad de Zaragoza, Zaragoza, Spain; MCZ, Museum of Comparative Zoology, Harvard University, Cambridge, USA; MUPA, Museo de Paleontología de Castilla-La Mancha, Cuenca, Spain; MZB, Museu Zoològic de Barcelona, Barcelona, Spain; NHMUK, Natural History Museum, London, UK; OUVC, Ohio University Vertebrate Collections, Athens, Ohio, USA; PIN, Borissiak Paleontological Institute, Russian Academy of Sciences, Moscow, Russia; QM, Queensland Museum, Brisbane, Queensland, Australia (F, fossil); STUS, Sala de las Tortugas 'Emiliano Jiménez' de la Universidad de Salamanca, Salamanca, Spain; TMM, Texas Memorial Museum, Austin, Texas, USA; UA, Université d'Antananarivo, Antananarivo, Madagascar; UF, University of Florida, Gainesville, Florida, USA; UMZC, University Museum of Zoology, Cambridge, UK; ZIN, Zoological Institute, Russian Academy of Sciences, Saint Petersburg, Russia; ZMMU MSU R, Zoological museum of Moscow State University, Moscow, Russia.

2.2 | Anatomical abbreviations

In order to simplify the manuscript reading, most of the time we have named the reconstructions of the internal cavities housing the soft tissues and organs as if they were these soft tissues themselves (e.g., inner ear instead of inner ear cavity, brain instead of endocast of the endocranial cavity, etc.). Also for simplicity, some

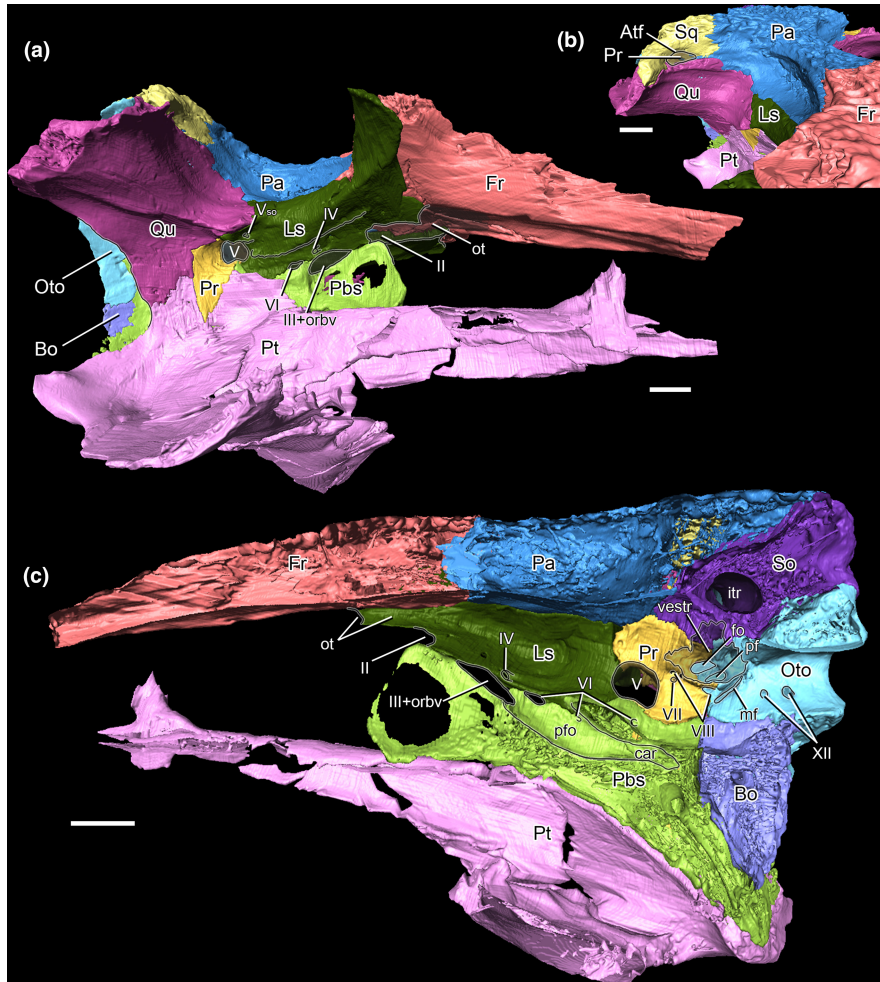


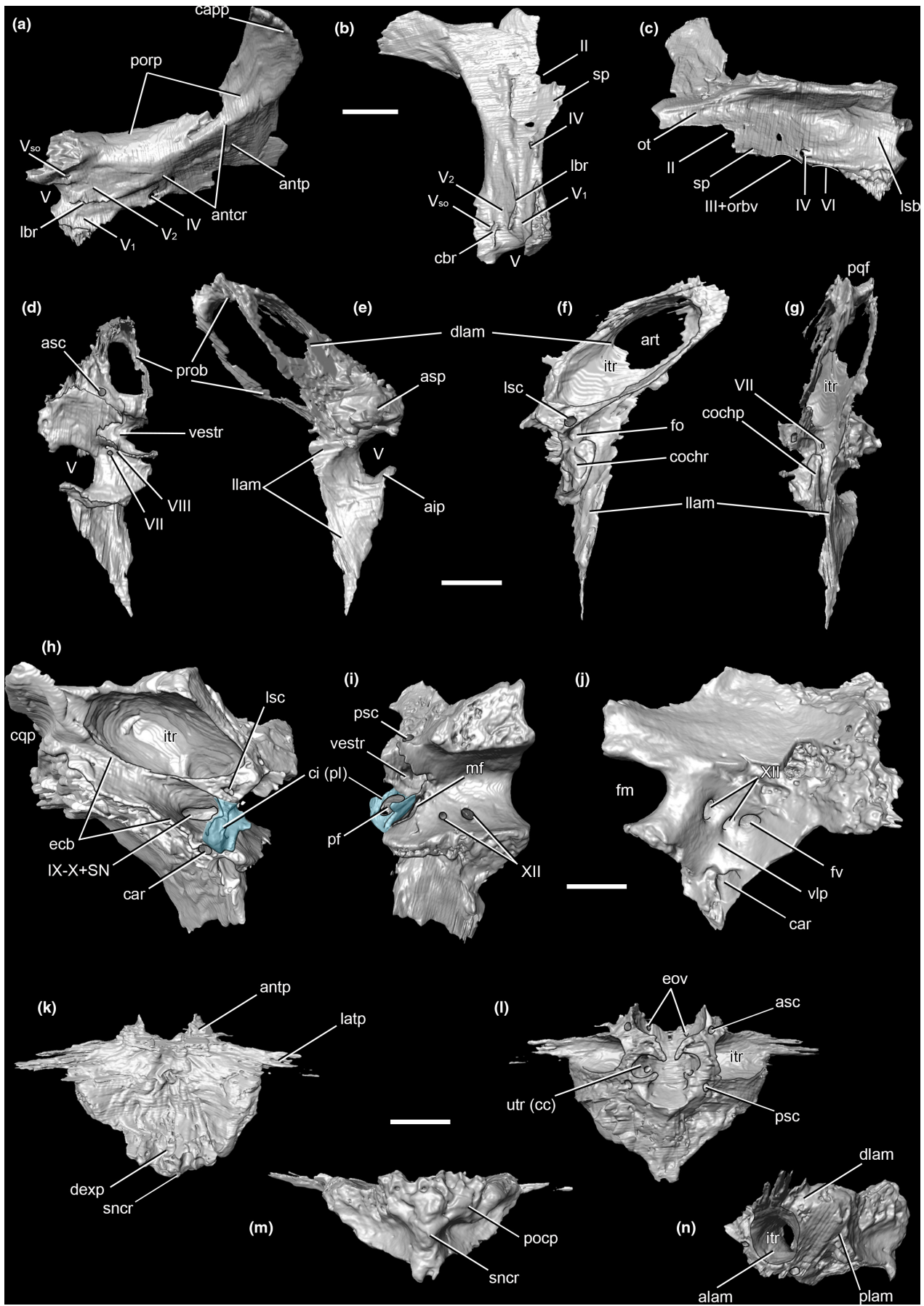
FIGURE 4 Three-dimensional detailed reconstruction of the neurocranium of *Portugalosuchus azenhae* (ML1818) in: right lateral view (a), with details of the braincase wall; right dorsolateral view (b), with details of the supratemporal fenestra region; and right medial view (c) showing the endocranial aspect of the braincase. Scale bar = 1 cm. For anatomical abbreviations, see Material and methods section. II, III, IV, V, VI, VII, VIII and XII refer to the nerves foramina and not to the cranial nerves themselves.

osteological correlates of the soft tissues (e.g., psc fo. = foramen of the posterior semicircular canal; V1 gr. = groove for the ophthalmic V1 nerve branch) have been left with the same abbreviation as the soft tissue cavity itself (e.g., psc. instead of psc fo., and V1 instead of V1 gr.).

aa., anterior ampula; **aip.**, anterior inferior process; **al.**, tooth alveolus; **alam.**, anterior lamina; **alp.**, alar process; **An.**, angular; **antcr.**, antotic crest; **antp.**, anterior process; **art.**, artificial gap of dorsal lamina; **asc.**, anterior semicircular canal; **asp.**, anterior superior process; **Atf.**, anterior temporal (= orbitotemporal) foramen; **Bo.**, basioccipital; **bof.**, basioccipital facet; **bopl.**, basioccipital plate; **bor.**, basioccipital recess; **Bs.**, basisphenoid; **bsd.**, basisphenoid diverticula; **capp.**, capitate process; **car.**, cerebral carotid artery; **cbr.**,

caudal bridge; **cc.**, common crus; **cd.**, cochlear duct; **cer.**, cerebrum; **cer hem.**, cerebral hemisphere; **CF.**, cephalic flexure angle; **cf.**, foramen caroticum; **ch.**, choana; **ci (pl).**, crista interfenestralis of the perilymphatic loop; **Co.**, coronoid; **cochp.**, cochlear prominence; **cochr.**, cochlear recess; **cqp.**, cranioquadrate passage; **dac.**, dorsal alveolar canal; **De.**, dentary; **dexp.**, dorsal exposure; **dlam.**, dorsal lamina; **Ec.**, ectopterygoid; **ecb.**, extracapsular buttress; **emf.**, external mandibular fenestra; **endo.**, endocranial surface; **eov.**, foramen for external occipital vein; **FIC.**, foramen intermandibularis caudalis; **FIM.**, foramen intermandibularis medius; **fm.**, foramen magnum; **fo.**, fenestra ovalis; **Fr.**, frontal; **fv.**, foramen vagi; **ie.**, inner ear; **II.**, optic cranial nerve; **III.**, oculomotor nerve; **IV.**, trochlear nerve; **itr.**, intertympanic pneumatic recess; **its.**, intertympanic

FIGURE 5 Three-dimensional detailed reconstructions of neurocranial bones of *Portugalosuchus azenhae* (ML1818). Right laterosphenoid in lateroventral (a), ventral (b), and medial (c) views. Right prootic in medial (d), lateral (e), posterior (f), and ventral (g) views. Right otoccipital (= exoccipital) in anterior (h), medial (i), and posterior (j) views. Supraoccipital in dorsal (k), ventral (l), posterior (m), and medial (n) views. Scale bar = 1 cm. For anatomical abbreviations, see Material and methods section. II, III, IV, V, VI, VII, VIII, IX and XII refer to the nerves foramina and not to the cranial nerves themselves.



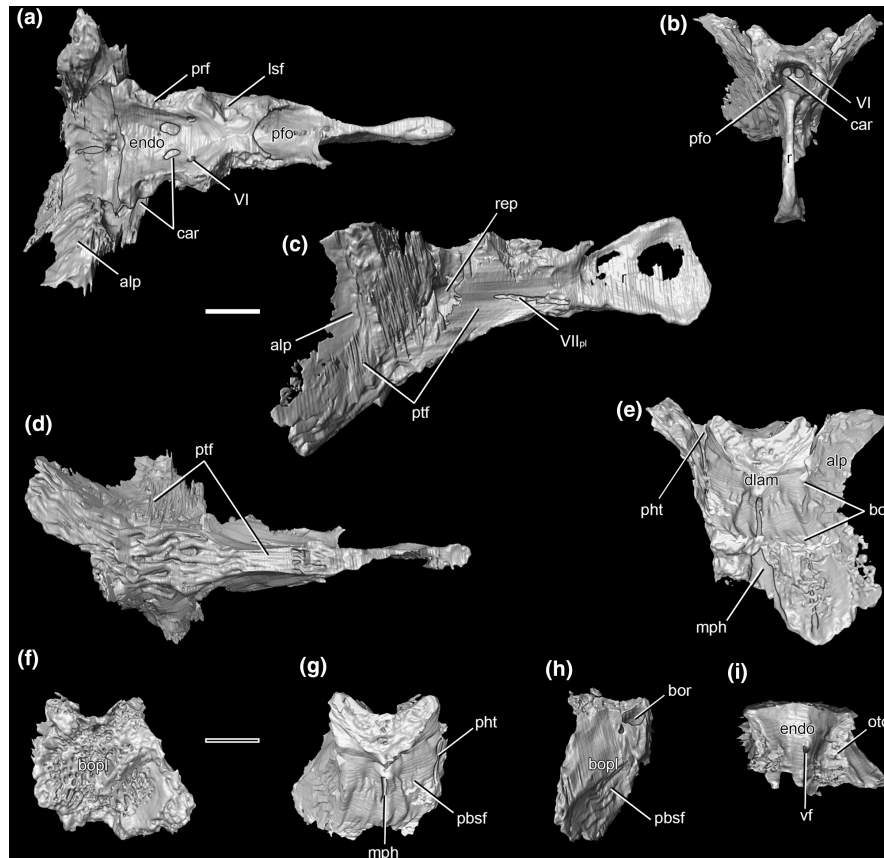


FIGURE 6 Three-dimensional detailed reconstructions of neurocranial bones of *Portugalosuchus azenhae* (ML1818). Basisphenoid in dorsal (a), anterior (b), right lateral (c), ventral (d), and posterior (e) views. Basioccipital in posterior (f), anterior (g), right lateral (h), and dorsal (i) views. Scale bar = 1 cm. For anatomical abbreviations, see Material and methods section. VI refer to the nerve foramen and not to the cranial nerve itself.

diverticula; **IX**, glossopharyngeal cranial nerve; **Ju.**, jugal; **juf.**, jugal foramen; **La.**, lachrymal; **latp.**, lateral process; **lbr.**, lateral bridge; **lef.**, lateral Eustachian canal; **llam.**, lateral lamina; **Ls.**, laterosphenoid; **lsb.**, laterosphenoid body; **lsc.**, lateral semicircular canal; **lsf.**, laterosphenoid facet; **mef.**, median Eustachian canal; **mf.** metotic foramen; **mph.**, median pharyngeal canal/foramen; **mpe.**, medial pharyngeal sinus; **Mx.**, maxilla; **nDO.**, dorsal branch of trigeminal nerve; **nld.**, nasolacrimal duct; **npd.**, nasopharyngeal duct; **nSO.**, supraorbital branch of trigeminal nerve (= **V_{so}**); **nTYM.**, tympanic branch of trigeminal nerve (= **V_{tym}**); **ob.**, olfactory bulb; **or.**, orbit; **orbv.**, orbital vasculature; **ornc.**, olfactory region of the nasal cavity; **ot.**, olfactory tract; **Oto.**, otoccipital; **otof.**, otoccipital facet; **Pa.**, parietal; **Pbs.**, parabasisphenoid; **pbsf.**, parabasisphenoid facet; **PF.**, pontine flexure angle; **Pf.**, prefrontal; **pf.**, perilymphatic foramen; **pfo.**, pituitary (hypophyseal) fossa; **Pl.**, palatine; **plam.**, posterior lamina; **Po.**, postorbital; **pocp.**, postoccipital process; **pqf.**, postquadrate foramen; **Pr.**, prootic; **prf.**, prootic facet; **psc.**, posterior semicircular canal; **mf.**, metotic foramen; **pht.**, groove of pharyngotympanic canals; **porp.**, postorbital process; **prob.**, prootic buttress; **Pt.**, pterygoid; **ptf.**, pterygoid facet; **pts.**, pharyngotympanic sinus; **ptt.**, pharyngotympanic tube; **Qu.**, quadrate; **rep.**, pneumatic recessus epitubaricus; **sa.**, sacculus; **si.**, siphonial tube; **SN.**, foramen for sympathetic nerve; **sncr.**, sagittal nuchal

crest; **Sq.**, squamosal; **So.**, supraoccipital; **Sp.**, splenial; **sp.**, slender process; **stf.**, supratemporal fenestra; **Su.**, surangular; **to.**, tooth; **utr (cc).**, utricular recess (crus communis); **V.**, trigeminal nerve; **V₁**, ophthalmic division of trigeminal nerve; **V₂**, maxillary division of trigeminal nerve; **V₃**, mandibular division of trigeminal nerve; **V_{so}**, supraorbital division of trigeminal nerve; **vestr.**, vestibular recess; **vf.**, vascular foramen; **VI.**, abducens nerve; **VII.**, facial nerve; **VII_{pl}**, foramen/groove for palatine branch of the facial nerve; **VIII.**, vestibulocochlear nerve; **vlp.**, ventrolateral process; **vls.**, ventral longitudinal sinus; **X.**, vagus cranial nerve; **XI.**, accessory cranial nerve; **XII.**, hypoglossal cranial nerve; **Xtym.**, canal for tympanic branch of vagus nerve.

3 | RESULTS AND DISCUSSION

3.1 | Systematic Paleontology

Crocodylomorpha Hay, 1930 (sensu Walker, 1970).

Crocodyliformes Hay, 1930.

Mesoeucrocodylia Whetstone & Whybrow, 1983.

Neosuchia Gervais, 1871 (sensu Benton & Clark, 1988).

Eusuchia Huxley, 1875.

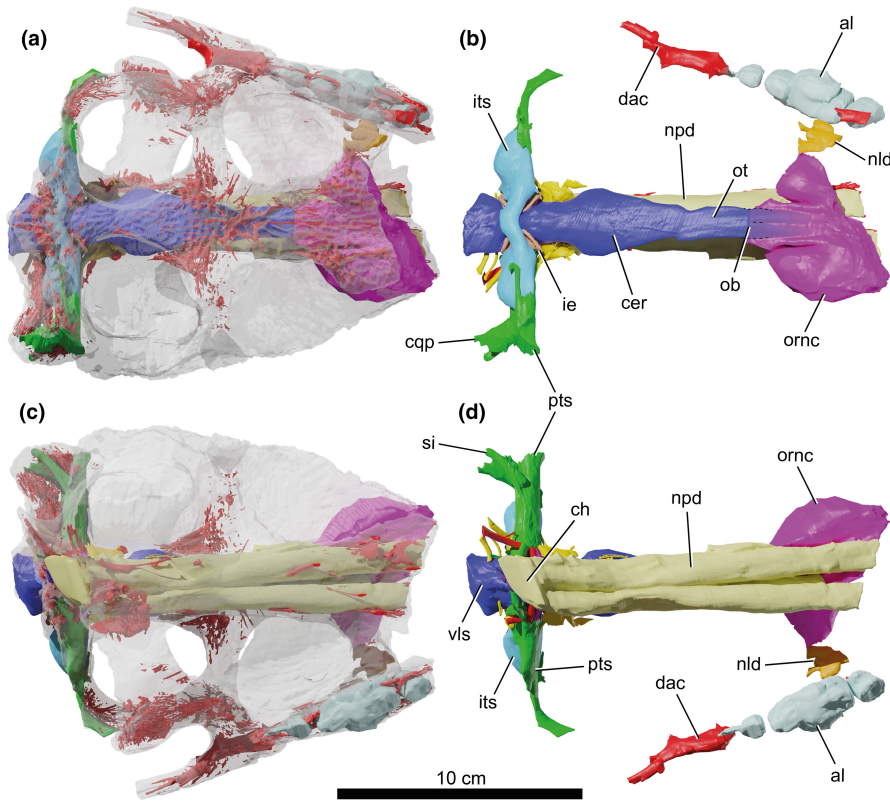


FIGURE 7 Three-dimensional reconstruction of the skull (with transparency) and cranial cavities (colored) of *Portugalosuchus azenhae* (ML1818) in dorsal (a, b), and ventral (c, d) views. For anatomical abbreviations, see Material and methods section.

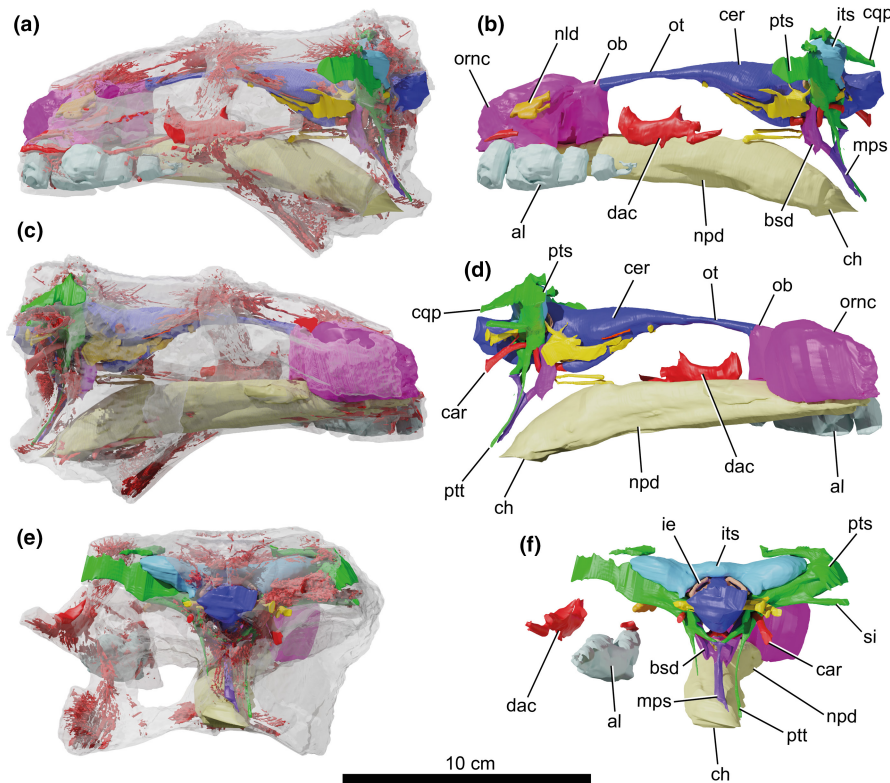


FIGURE 8 Three-dimensional reconstruction of the skull (with transparency) and cranial cavities (colored) of *Portugalosuchus azenhae* (ML1818) in left lateral (a, b), right lateral (c, d), and posterior (e, f) views. For anatomical abbreviations, see Material and methods section.

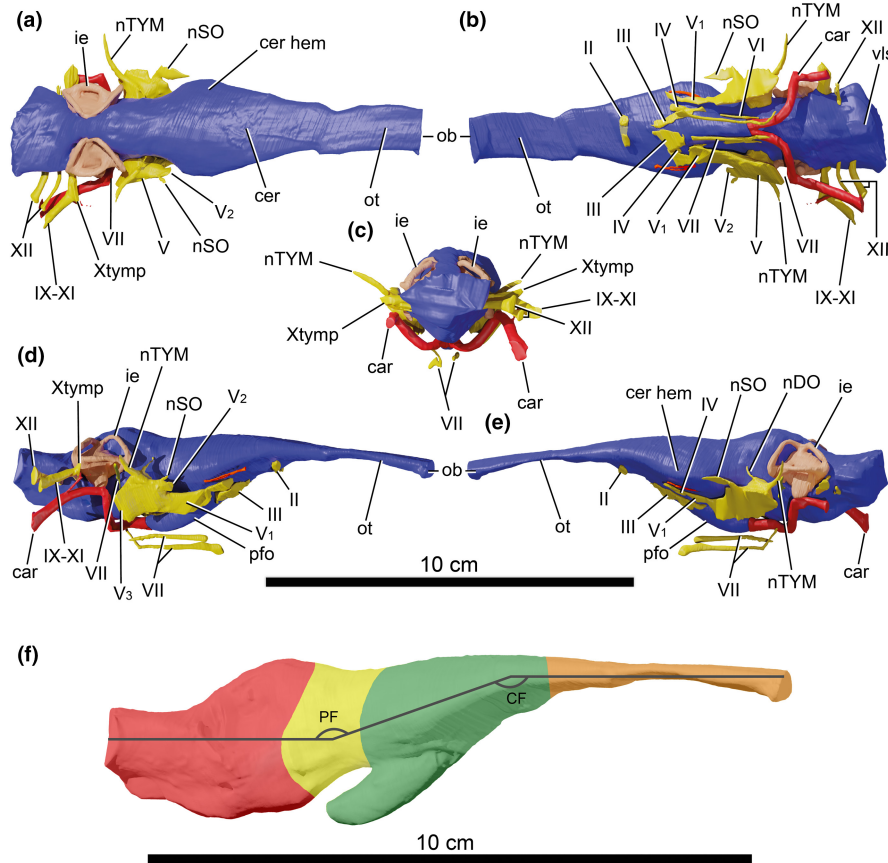


FIGURE 9 Three-dimensional detailed reconstruction of the neurocranial cavities of *Portugalosuchus azenhae* (ML1818) in: dorsal (a), ventral (b), posterior (c), right lateral (d), and left lateral (e). Major brain divisions in right lateral view: hindbrain (red), midbrain (yellow), forebrain (green), and olfactory tract (orange). For anatomical abbreviations, see Material and methods section.

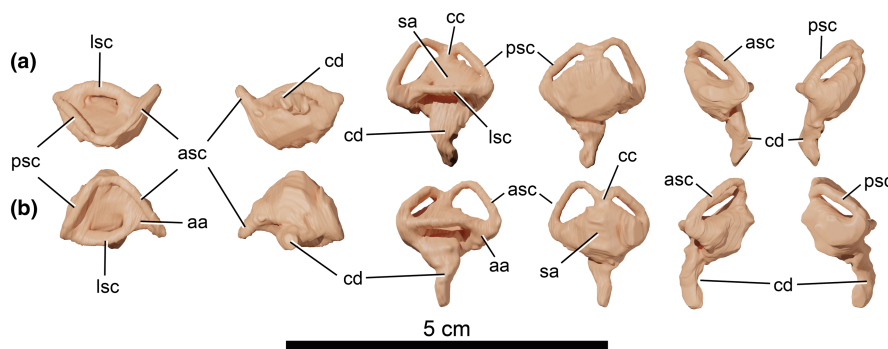


FIGURE 10 Three-dimensional detailed reconstruction of the left (a) and right (b) inner ear cavities of *Portugalosuchus azenhae* (ML1818) in dorsal, ventral, lateral, medial, anterior, and posterior views respectively. For anatomical abbreviations, see Material and methods section.

Crocodylia Owen, 1842 (sensu Benton & Clark, 1988).

Portugalosuchus Mateus et al. (2019).

Portugalosuchus azenhae Mateus et al. (2019).

Holotype: Partial skull and mandible (ML1818) (Figures 1 and 3).

Age and Horizon: Lower member of Tentúgal Formation, Upper Cenomanian, Late Cretaceous (about 95 Myr).

Type Location: Limestone quarry of Casal dos Carecos, near Tentúgal, Portugal.

3.1.1 | Emended diagnosis

Same diagnosis for the genus and the species by monotypy. Thanks to the new data obtained from the CT scan, some characters have been reinterpreted, the phylogenetic position has changed, and the diagnosis of genus and species have been modified accordingly. *Portugalosuchus azenhae* is characterized by the following autapomorphies: external mandibular fenestra located at the

dentary-angular suture, with a posterior process of the dentary forming its anterior and dorsal margins, the angular forming its posterior and ventral margins, and without the participation of the surangular in the fenestra; dorsal margin of the infratemporal fenestra very elongated, with the quadratojugal contacting the base of the skull table posteriorly, giving a trapezoidal contour to the fenestra (rather than triangular); and huge prootic exposure on the external lateral braincase wall, with a moderate dorsal exposure and a large subsubtriangular ventral exposure that wedges ventrally between the pterygoid. It is also characterized by the unique combination of unambiguous synapomorphies: posterolateral edges of the skull table planar or horizontal across their entire length; presence of a subtle midsagittal crest on the fused frontals between the orbits; presence of foramina in the posteromedial wall of the supratemporal fenestra; concavity on the ventral margin of the basioccipital, posterior to median eustachian foramen; lateral eustachian foramina at the same level or height of the median eustachian foramen; and large dorsoventral exposure of the basisphenoid ventral to the basioccipital, in posterior view.

3.2 | Skull anatomy of *Portugalosuchus*

3.2.1 | General comments

The cranial osteology of *Portugalosuchus* (ML1818) has been originally described in Mateus et al. (2019). The CT-scanning and 3D modelling of this specimen made herein overall confirm the initial description and the suggested sutural patterns. However, these techniques allow a detailed description of the largely complete and undistorted neurocranium of ML1818, as well as several additional observations on other parts of the skull to supplement or correct the original account by Mateus et al. (2019). Osteological terminology used herein follows Lordansky (1973) and Kuzmin et al. (2021).

Both prefrontal pillars of *Portugalosuchus* are complete and contact ventrally with the pterygoids and likely palatines (Figure 2d,e). Due to breakage in this area, the contact between the pterygoid and palatine is hard to establish in ML1818, and the base of each prefrontal pillar has been segmented as a part of the pterygoid. However, in extant crocodylians, the palatines considerably participate in the base of these pillars and contact the prefrontals (e.g., Lordansky, 1973: Figure 6), a condition expected in *Portugalosuchus* but not presently confirmed. The dorsal half of each prefrontal pillar is anteroposteriorly expanded and transversally narrow. Both medial processes are present and approach each other medially (Figure 2e). The medial processes of *Portugalosuchus* are anteroposteriorly expanded and somewhat constricted laterally at their bases. Each medial process of the prefrontal pillar is nearly twice as long anteroposteriorly as deep dorsoventrally. The prefrontal pillar is solid internally.

The jugal, while being crushed and slightly incomplete, appears to be more anteriorly extended than previously reconstructed (see Figure 3a,d in Mateus et al., 2019). It wedges between the maxilla

and the lacrimal and separates these elements for most of their preserved length; only a brief contact between the maxilla and the lacrimal seems to exist anteromedially (Figure 2a,c). The jugal contains a large neurovascular recess internally below the postorbital bar. This recess opens posteriorly via the large posterodorsal jugal foramen and medially via the apparently large medial jugal foramen. The lateromedial width of the posterodorsal foramen is at least half the width of the postorbital bar in posterior view (juf in Figure 2f). The medial jugal foramen is incomplete due to crushing; however, its posterior margin is sufficiently preserved to infer that its size was approximately equal to that of the posterodorsal jugal foramen.

The sutural pattern on the ventral surface of the postorbital-squamosal bar differs from that initially described in *Portugalosuchus* (see Figure 6a,b in Mateus et al., 2019). Neither quadrate nor quadratojugal contacts the postorbital ventrally on the postorbital-squamosal bar based on the CT data of ML1818 (see three-dimensional models in Supplementary Information S3).

3.2.2 | Neurocranial osteology

The neurocranium of ML1818 is well-preserved, with only small portions of the parabasisphenoid rostrum, both paroccipital processes of the otoccipitals, and the posterior portion of the basioccipital being absent (Figures 2 and 4). The left pharyngotympanic (middle ear) cavity is exposed in posterior view due to the breakage of the specimen (Figure 2f). Both meatal chambers (= outer ear cavities; Montefeltro et al., 2016) are partially preserved. On the left side of ML1818, a depression formed by the squamosal and quadrate marks the anterior corner of the meatal chamber and the external auditory meatus (Figure 2c). On the right side, the external auditory meatus, the cranioquadrate passage, and the vascular postquadrate foramen are exposed (Figure 2d). However, it is impossible to infer the sutural relationships between the quadrate and the squamosal posterior to the external auditory meatus due to imperfect preservation. Thus, it remains unknown whether the cranioquadrate passage in *Portugalosuchus* was dorsally open, as in most noncrocodylian eusuchians (e.g., *Agaresuchus*, *Allodaposuchus*, *Hylaeochampsa*, *Iharkutosuchus*, *Lohuecosuchus*), or closed as in crown-group crocodylians and eusuchian *Isisfordia* (Hart et al., 2019; Salisbury et al., 2006). The ventral margin of the external auditory meatus lies ventral to the level of the dorsal margin of the infratemporal fenestra, as in most eusuchians (Rio & Mannion, 2021).

The temporal canal is completely preserved on the right side of ML1818 (see Neuroanatomy section). As in extant crocodylians (see Walker, 1990; Kuzmin et al., 2021: Figure 5), the temporal canal of *Portugalosuchus* opens anteriorly, into the supratemporal fossa by the anterior temporal (= orbitotemporal) foramen, posteriorly on the occipital surface by the post-temporal fenestra, and is connected to the cranioquadrate passage and the external auditory meatus by the postquadrate foramen laterally. The ventral margin of the anterior temporal foramen is completely formed by the quadrate that separates the parietal and

the squamosal (Figure 4b). This differs from the condition in basal (e.g., *Diplocynodon*) and derived alligatoroids (e.g., *Alligator*, *Caiman*, *Melanosuchus*), in which the parietal and squamosal either approach or directly contact each other and separate the quadrate from the ventral border of the anterior temporal foramen (e.g., Brochu, 1997a, 1999; Rio & Mannion, 2021). In *Portugalosuchus*, the squamosal-parietal contact passes medially to the anterior temporal foramen, as in *Thoracosaurus isorynchus* (Rio & Mannion, 2021) and *T. borissiakii* (CCMGE 1/3373). The floor of the temporal canal is formed mostly by the prootic, with a small addition of the supraoccipital medially (Figure 4b). This is consistent with most basal eusuchians and closely related taxa: e.g., *Isisfordia* (Hart et al., 2019), *Paralligator* (PIN 554-1, PIN 3141/501), alligatoroids *Alligator* and *Diplocynodon* (figure 30 in Rio et al., 2020), and the gavialoid *T. borissiakii* (CCMGE 1/3373). Among crown-group crocodylians, *Caiman*, *Crocodylus*, *Gavialis*, *Mecistops*, *Osteolaemus*, and *Tomistoma* have the narrower exposure of the prootic on the floor of the temporal canal (Kuzmin et al., 2021).

The orbitotemporal region of the neurocranium is represented by a pair of completely ossified laterosphenoids (Figures 2, 4 and 5). The laterosphenoid of *Portugalosuchus* is extremely anteroposteriorly elongated. It is subdivided into the shorter anterior (orbital) and longer posterior (temporal) aspects by a prominent arched antotic crest (Figure 5a). The orbital aspect of the laterosphenoid is a flat ventrally oriented surface formed by the anterior and slender processes (Figures 4a and 5a). The anterior process is relatively short; its anterior margin is perpendicular to the sagittal plane and lies at the same level as the capitate process (Figure 5a,b). This condition is also observed in most gavialoids and certain tomistomines among eusuchians: e.g., *Gavialis*, *Eogavialis*, *Maroccosuchus*, *Paratomistoma*, *Piscogavialis*, *Thecachampsas*, *Thoracosaurus* (Brochu, 1997a, 1999; Brochu & Gingerich, 2000; Jouve et al., 2015; Kuzmin et al., 2021; Rio & Mannion, 2021). The anterior processes approach each other medially but without making a contact. Together with the frontal, they surround the foramen for the olfactory tract (Figure 4a). The olfactory tract extends anteriorly within the limits of a shallow groove on the ventral surface of the frontal (see Neuroanatomy section). Posterior to the foramen for the olfactory tract, a short slender process extends medially from each of the laterosphenoids (Figures 4a,c and 5a-c). These processes contact the anterodorsal tip of the parabasisphenoid rostrum and form the foramen for the optic cranial nerve (CN II). Just posterior to the slender process, a large foramen is formed on both sides of the braincase between the laterosphenoid and parabasisphenoid rostrum (Figure 4a). The oculomotor (CN III) cranial nerve and orbital vasculature passed from the braincase and the hypophyseal cavity into the orbit via these foramina in *Portugalosuchus*, as in extant crocodylians (Kuzmin et al., 2021; see Neuroanatomy section). On the right side of ML1818, a small opening is posteriorly delimited from this larger foramen by the additional laterosphenoid-parabasisphenoid contact (Figure 4a,c). This smaller foramen might represent a separate passage for abducens nerve (CN VI) into the orbit. The trochlear nerve (CN IV) passes entirely

through the anterior process of the laterosphenoid just dorsal to the large foramen for CN III and associated vasculature (Figures 4 and 5).

The temporal aspect of the laterosphenoid is formed by the elongated postorbital and capitate processes (Figure 5a). The capitate process projects perpendicular to the sagittal plane and fits into a socket on the ventral surface of the postorbital. The postorbital process forms the medial wall of the supratemporal fossa and likely was the main site for the attachment of *M. pseudotemporalis superficialis* (e.g., Holliday et al., 2013; Holliday & Witmer, 2009; Lessner & Holliday, 2022). Ventrally to the postorbital process, the laterosphenoid body forms the anterior half of the large trigeminal (= maxillo-mandibular) foramen for the exit of the trigeminal cranial nerve (CN V) and bears grooves for its main branches: the ophthalmic (CN V₁) and maxillary (CN V₂) nerves (Figures 4 and 5). The lateral bridge of the laterosphenoid is incomplete and reduced on both sides of ML1818 to a very short process directed ventrally (Figure 5a,b). The reduced lateral bridge of the laterosphenoid is known in the eusuchian *Hylaeochampsas*, as also in certain gavialoids and crocodyloids: e.g., *Gavialis*, *Gryposuchus*, *Eogavialis*, *Mecistops*, *Paratomistoma*, *Piscogavialis*, *Osteolaemus*, and *Tomistoma* (Holliday & Witmer, 2009; Kuzmin et al., 2021; Rio & Mannion, 2021). A tiny caudal bridge is present near the contact of the laterosphenoid and quadrate on the right side of ML1818 (Figures 4a and 5a,b); it delimits a short passage for the supraorbital branch of the trigeminal nerve (CN V_{so} or nSO) (see Neuroanatomy section).

The lateral wall of the braincase is completely preserved on the right side of ML1818 and slightly damaged posteriorly on its left side (Figures 2c,d and 4a). The large trigeminal (= maxillo-mandibular) foramen is formed by the laterosphenoid anteriorly, the quadrate dorsally, and the prootic posteriorly and ventrally. The sutural relationships on the lateral wall of the braincase, as inferred from the CT scans of ML1818, differ slightly from the initial interpretation in Mateus et al. (Mateus et al., 2019: Figure 9). The lateral lamina of the prootic has an extensive external exposure posterior and ventral to the trigeminal foramen and contacts the pterygoid (Figure 4a), as in fossil *Thoracosaurus* (CCMGE 1/3373) and extant *Gavialis* and *Tomistoma* (Kuzmin et al., 2021). Accordingly, the laterosphenoid and quadrate contact each other dorsally to the trigeminal foramen but not ventral to it. Among studied neosuchians, the prootic-ptyergoid contact ventral to the trigeminal foramen is present in alligatoroids *Alligator*, *Caiman*, *Diplocynodon*, gavialoids *Thoracosaurus* (CCMGE 1/3373) and *Gavialis*, and tomistomines *Paratomistoma* and *Tomistoma* (Brochu & Gingerich, 2000; Kuzmin et al., 2021; Serrano-Martínez et al., 2019b). The prootic of *Portugalosuchus* forms the posterior and most of the dorsal and ventral limits of the trigeminal fossa. The dorsal surface of the trigeminal fossa is pierced by the canal for the connection of the sympathetic nerve (SN) with the trigeminal ganglion (see Bellairs & Shute, 1953: text-Figure 5; Lessner & Holliday, 2022: Figure 6; Kuzmin et al., 2021). This is frequently referred to as the tympanic branch of CN V (V_{tym} or nTYM). This canal extends from the pharyngotympanic (middle ear) cavity to the trigeminal fossa (see Neuroanatomy).

As in extant crocodylians, the prootic of *Portugalosuchus* may be subdivided into the capsular portion, the superior and inferior anterior processes, the lateral and dorsal laminae, and the prootic buttress (Figure 5d–g). The two anterior processes (superior and inferior) bound the trigeminal fossa (see above). The lateral lamina is a lateromedially thin but dorsoventrally extensive process that is nearly parallel to the sagittal plane. It covers the capsular portion of the prootic and the foramen for the facial cranial nerve (CN VII) in lateral aspect and is exposed on the lateral wall of the braincase posterior to the trigeminal foramen (Figures 4a and 5g). Dorsally, the lateral lamina is continuous with the lateromedially expansive but anteroposteriorly thin dorsal lamina that is perpendicular to the sagittal plane (Figure 5e,f). Both laminae extensively suture to the quadrate and internally form the surface of the pharyngotympanic (middle ear) cavity and its pneumatic outgrowth. This can be clearly observed on the left side of the skull due to the breakage that exposed the pharyngotympanic cavity in posterior view (Figure 2f). The dorsal laminae are incompletely segmented on both sides of ML1818 leaving a large artificial gap in each (Figure 5f); this is due to a tight contact with the corresponding quadrate and lack of resolution in CT scans in this region. The dorsal lamina is continuous posteriorly with the prootic buttress. The prootic buttress forms a thin loop around the intertympanic pneumatic recess and extends between the dorsal lamina and the capsular portion of the prootic (Figure 5d–g). The prootic buttress sutures to the parietal dorsally, to the supraoccipital dorsomedially, and to the otoccipital posteriorly. It forms part of the floor of the temporal canal and divides the supraoccipital and quadrate there (Figure 4b).

Each otic capsule is formed by the prootic, the otoccipital, and the supraoccipital (Figure 5c). The otic bullae are missing their medial (endocranial) walls; otherwise, otic capsules are essentially complete and reconstructed in detail. The anatomy of the otic and periotic region of *Portugalosuchus* is similar to that of extant crocodylians (e.g., Kuzmin et al., 2021; Walker, 1990) and contrasts with the enlarged and medially merging otic capsules of dyrosaurids (e.g., Erb & Turner, 2021). The prootic forms the anterior third of the otic capsule (Figure 4c). It encloses the anterior portion of the vestibular recess and the anterior and lateral semicircular canals (Figure 5d,f). The posterior portion of the vestibular recess and the posterior and lateral semicircular canals are housed within the otoccipital, while the supraoccipital comprises dorsal routes of the anterior and posterior semicircular canals and their common crus (utricle recess) (Figures 4c and 5). The prootic and the otoccipital together form the lateral bulge (cochlear prominence; Figure 5g) that projects into the pharyngotympanic cavity and contained the cochlear duct of the inner ear and the perilymphatic cisterns that surrounded it (e.g., see figure 12 in Kuzmin et al., 2021). The fenestra ovalis, which received the footplate of the stapes, is bounded by the prootic anteriorly and the otoccipital posteriorly, while the fenestra pseudorotunda (for compensatory secondary tympanic membrane) is bordered solely by the otoccipital. These two fenestrae are divided by a thin crista interfenestralis of the perilymphatic loop (Figures 4c and 5h,i). The

latter is a thin process formed by the otoccipital that coils around the perilymphatic foramen and makes the suture of the otoccipital with itself (loop-closure suture; see Walker, 1990; Kuzmin et al., 2021).

The periotic region is located within the otoccipital (= exoccipital in many previous accounts, see Kuzmin et al., 2021). It is complete on the right side of ML1818 and partially preserved on the left side of the specimen. An oblique concave bony lamina termed the extracapsular buttress (previously referred to as subcapsular process or subcapsular buttress, see Kuzmin et al., 2021) extends between the otic capsule ventromedially and the cranioquadrate passage dorsolaterally (Figure 5h). Its medial portion, which is adjacent to the otic capsule, contains the space termed the recessus scalae tympani. It housed the perilymphatic sac, the glossopharyngeal (CN IX) and vagus (CN X) cranial nerves, the sympathetic nerve (SN), and associated vasculature (Kuzmin et al., 2021; Lessner & Holliday, 2022) (see Neuroanatomy). In ML1818, the internal opening for CN IX, X, and SN is a single continuous groove on the posterior surface of the extracapsular buttress (Figure 5h); however, in extant crocodylians, there are usually three separate foramina in this region (e.g., Kuzmin et al., 2021). This neurovascular groove extends laterally from the metotic foramen to the common neurovascular canal within the otoccipital. In *Portugalosuchus*, the metotic foramen is a narrow fissure located on the endocranial surface posterior to the otic capsule (Figures 4c and 5i). In extant crocodylians, it provides the passage for CN IX and X out of the endocranial cavity (Iordansky, 1973; Kuzmin et al., 2021; Lessner & Holliday, 2022; Walker, 1990). The common neurovascular canal for CN IX, X, SN, and associated vessels pierces the otoccipital of *Portugalosuchus* and opens by a large foramen vagus on its posterior surface (Figures 2g and 5j). The canal for the cerebral carotid artery opens on the posterior surface of the otoccipital ventral to the foramen vagi. The two foramina are notably separated in *Portugalosuchus*, whereas they are closely spaced in some gavialoids: e.g., *Gavialis*, *Gryposuchus*, *Eogavialis*, *Piscogavialis*, and *Thoracosaurus* (CCMGE 1/3373; see Rio & Mannion, 2021: character 126). The posterior foramen of the cerebral carotid artery is located at the same level as the dorsal tip of the parabasisphenoid (“lateral to the parabasisphenoid”), as in most studied neosuchians but differing from extant *Crocodylus*, *Mecistops*, *Osteolaemus*, and *Tomistoma* (see Brochu, 1997a, 1999; Kuzmin et al., 2021). The anterior opening of the cerebral carotid canal is located just ventral to the otic capsule and the extracapsular buttress (Figure 5h). Dorsolaterally, the extracapsular buttress passes to the cranioquadrate passage. The floor of the cranioquadrate passage is formed both by the otoccipital and the quadrate in *Portugalosuchus* (Figure 2d). This is consistent with the condition of the studied crown-group crocodylians and the eusuchian *Isisfordia* (Hart et al., 2019; Iordansky, 1973; Kuzmin et al., 2021; Salisbury et al., 2006) but differs from most noncrocodylian neosuchians (e.g., *Allodaposuchus*, *Bernissartia*, *Lohuecosuchus*, *Hylaeochampsia*, *Kansajsuchus*, *Paralligator*), which lack the quadrate participation to the cranioquadrate passage (see Kuzmin et al., 2019; Martin et al., 2020; Narváez et al., 2015, 2020).

Both paroccipital processes are lacking in ML1818. However, the ventrolateral process of the more complete right otoccipital is

present (Figure 5j). It is a transversely extensive bony lamina that contacts the basioccipital ventrally, the parabasisphenoid anteroventrally, and the quadrate anterodorsally. The otoccipital does not extend far ventrally at the contact with the basioccipital tuberosities (Figure 2f), as in most eusuchians except some gavialoids (e.g., *Gavialis*, *Eogavialis*, *Gryposuchus*: Brochu, 1997a, 1999; Rio & Mannion, 2021). The occipital arch of each otoccipital sutures ventrally to the basioccipital and dorsally to the supraoccipital and the contralateral otoccipital. It forms the dorsal and lateral margins of the foramen magnum and is pierced by a pair of foramina for hypoglossal cranial nerve (CN XII) on the more complete right side of ML1818 (Figure 5j).

The supraoccipital is a small unpaired element that participates in the otic capsules and the posterior (occipital) surface of the skull of *Portugalosuchus*. The bone is notably dorsoventrally compressed; its lateromedial width on the occiput and the anteroposterior length in dorsal view are twice the dorsoventral depth (Figures 4c and 5k-n). It has a small exposure on the dorsal surface of the skull table just posterior to the parietal (Figures 2a and 5k). As in extant crocodylians, the supraoccipital of *Portugalosuchus* may be subdivided into three portions – namely, the anterior, posterior, and dorsal laminae surrounding the pneumatic intertympanic recess (Figure 5n). The posterior lamina is exposed on the occipital surface of the skull and has paired postoccipital processes and the vertical sagittal nuchal crest (Figure 5m). The sagittal nuchal crest is very prominent in *Portugalosuchus*; it projects posteriorly beyond the level of the parietal and the postoccipital processes and is visible in dorsal view, as in extant caimanines, crocodyloids (except *Tomistoma*) and *Gavialis* (Kuzmin et al., 2021). The postoccipital processes are coalescent with the sagittal nuchal crest. They are not visible in dorsal view. Paired depressions are located on each side of the sagittal nuchal crest. The anterior lamina of the supraoccipital forms the concave dorsal surface of the endocranial cavity and participates in both otic capsules (Figure 5l). It contacts with the prootics anteroventrally and with the otoccipitals posteroventrally (Figure 4c). The dorsal lamina of the supraoccipital sutures to the parietal dorsally and the prootics laterally. Notable lateral processes project from each side of the supraoccipital of *Portugalosuchus* and participate in the floor of the temporal canal (Figure 5k); similar lateral projections are present in *Gavialis* among extant crocodylians. The pneumatic foramina are lacking in the dorsal lamina.

The ventral part of the neurocranium of *Portugalosuchus* is formed by the parabasisphenoid anteriorly and the basioccipital posteriorly (Figure 4c). Both these elements are dorsoventrally deep (verticalized) suggesting that ML1818 corresponds to an adult individual past the cranial metamorphosis sensu Tarsitano (1985) (see also Dufeu & Witmer, 2015; Kuzmin et al., 2021). The basioccipital is incompletely preserved lacking the entire occipital condyle and most of the posterior surface (Figures 2 and 6). The basioccipital plate projects ventrally from the endocranial surface formed by the basioccipital (Figure 6f,h). The anterior surface of the basioccipital plate contacts the parabasisphenoid and slopes slightly

posteroventrally (Figures 4c and 6h). Its preserved posterior aspect is vertical and faces posteriorly. As seen on the better-preserved right side of ML1818, the lateral margins of the basioccipital plate flare ventrally in *Portugalosuchus* (Figure 6f), as in some gavialoids like *Gavialis*, *Eogavialis*, and *Piscogavialis* (Jouve et al., 2008; Rio & Mannion, 2021). The basioccipital forms the posterior walls of the pneumatic pharyngotympanic (lateral Eustachian) canals and the median pharyngeal (median Eustachian) canal (Figure 6g; see Neuroanatomy). The external (ventral) foramina of the pharyngotympanic canals are located dorsally relative to the median pharyngeal foramen. The ventral margin of the basioccipital is concave posterior to the median pharyngeal foramen (Figures 2g and 6f). The apparently vascular canal for occipital veins (see Kuzmin et al., 2021; Owen, 1850) pierces the basioccipital plate and opens dorsally on the endocranial surface via a small single foramen (Figure 6i).

The parabasisphenoid (or simply basisphenoid in many previous accounts, see Kuzmin et al., 2021) is well-preserved in ML1818. It is notably elongated (anteroposterior length almost twice dorsoventral depth) and verticalized (Figure 4c and 6). Half of its length corresponds to the prominent rostrum or cultriform process. As in all crocodyliforms up to our knowledge, the anterior part of the rostrum of *Portugalosuchus* is dorsoventrally expanded, lateromedially thin and blunt (Figure 6c). As is seen on the better-preserved right side of ML1818, its lateral surface is smooth and devoid of a crescentic ridge present in some alligatoroids (character 203 in Rio & Mannion, 2021). The rostrum contacts the slender processes of both laterosphenoids at its anterodorsal tip and forms the ventral margins of the foramina for CN III, CN VI, and orbital vasculature posterior to this contact (Figure 4a). It becomes twice lateromedially wider ventral to the hypophyseal cavity than at its anterior terminus (Figure 6a,d). Just anterior to this widened part, a shallow sulcus is located on each side of the rostrum, although not as deep as that seen in other crocodylians such as *Gavialis* or *Alligator*. Posteriorly, the parabasisphenoid of *Portugalosuchus* smoothly merges with the lateral wall of its braincase but has no further external exposure ventral to the laterosphenoid; thus, the laterosphenoid-pterygoid contact is anteroposteriorly continuous (Figures 4a and 6c).

The hypophyseal (pituitary) cavity is rounded in cross-section, oriented horizontally, and anteroposteriorly extended (Figures 4c and 6a,b). Paired canals of the cerebral carotid arteries enter the cavity at its posterior-most terminus, and the small canals of the abducens nerve (CN VI) open on the dorsolateral walls within the limits of the hypophyseal cavity (Figures 4c and 6). Each cerebral carotid artery enters the parabasisphenoid dorsolaterally, has a sigmoidal course through its body, and passes into the hypophyseal cavity anteriorly. Two foramina on the endocranial surface of the parabasisphenoid correspond to unossified portions of the cerebral carotid canals (Figure 6a); these are generally absent in most crocodylians examined (e.g., Kuzmin et al., 2021: figure 19). CN VI pierce the endocranial surface of the parabasisphenoid anterolaterally to the abovementioned unossified gaps, exit the bone on the lateral walls of the hypophyseal cavity, and extend into the orbits via the foramina between the rostrum and the laterosphenoid (Figures 4c

and 6; see Neuroanatomy below and Lessner & Holliday, 2022). The palatine branches of the facial nerve (CN VII_p) extend ventrally in canals between the parabasisphenoid and the pterygoid and exit via paired foramina ventrolateral to the rostrum (Figure 6c; see Neuroanatomy).

The body of the parabasisphenoid forms the concave endocranial surface and is hollowed out by the pneumatic median pharyngeal recess and its lateral diverticula – the parabasisphenoid recesses (see Neuroanatomy). The pneumatic recessus epitubaricus is formed just lateral on each side of the parabasisphenoid body, at the connection between the pharyngotympanic (middle ear) cavity and the median pharyngeal recess (Figure 6c). The parabasisphenoid of *Portugalosuchus* contacts the laterosphenoid and the prootic dorsally and is tightly sutured to the pterygoids lateroventrally. The posterior surface of the parabasisphenoid (descending lamina sensu Kuzmin et al., 2021) slopes posteroventrally and contacts the basioccipital (Figure 6e). The parabasisphenoid is significantly exposed on the posterior (occipital) surface of the skull ventral to the basioccipital (Figure 2f), as in some noncrown-group neosuchians (e.g., *Agaresuchus fontisensis*, *Allodaposuchus precedens*, *Hylaeochampsa*, *Paralligator*) and extant *Alligator* but differing from the almost unexposed parabasisphenoid of most gavialoids (e.g., *Gavialis*, *Gryposuchus*, *Eogavialis*, *Thoracosaurus*). The exposure on the palate between the pterygoid and basioccipital is anteroposteriorly short and narrow (Figure 2b), also differing from the broader exposure in gavialoids (see Brochu, 1997a, 1999; Rio & Mannion, 2021). The paired alar processes project posterolaterally from the body of the parabasisphenoid. They are moderately exposed on the lateral wall of the braincase between the pterygoid, quadrate, otoccipital, and basioccipital (Figures 2 and 4a).

3.3 | Neuroanatomy of *Portugalosuchus*

Thanks to the excellent preservation of the skull of *Portugalosuchus* (ML1818), it was possible to reconstruct the olfactory region, olfactory bulbs, the posterior region of the nasopharyngeal ducts, brain, cranial nerves, carotid arteries, blood vessels, paratympanic sinus system and inner ear (Figures 7–10). The only cavities that could not be reconstructed are those found in the snout, as this part of the skull has not been preserved.

3.3.1 | Nasal cavity and associated structures

As most of the snout has not been preserved, only the posterior portion of the olfactory region, part of the nasolacrimal duct, the olfactory bulbs and the nasopharyngeal ducts could be reconstructed.

The olfactory region is an expanded chamber of the nasal cavity located anteromedially and ventral to the orbits, limited dorsally by the frontal and prefrontals, ventrally by the palatines,

posteromedially by the prefrontal pillars and posteriorly, and along the sagittal axis, by the olfactory bulbs (dark pink color in Figures 7 and 8). Posterolaterally, this cavity divides into two bilateral dorsally rounded chambers that develop in front of the orbits and laterally to the prefrontal pillars. Posteromedially, when the olfactory region passes between the prefrontal pillars, it is partially divided into a big trapezoidal dorsal cavity and a smaller rhombic shape ventral cavity due to the approximation of the medial processes of the pillars. The division of the chamber is not complete as the medial processes of the pillars do not get to contact each other. The posterior contact with the olfactory bulbs occurs between the pillars, at the dorsomedial area of the olfactory region (Figure 7a,b). This dorsomedial area forms an anteroposteriorly elongated sagittal shelf with elevated lateral margins with the two lobes of the olfactory bulbs placed between them (Figure 7b). These elevated lateral margins run parallel until they reach the olfactory tract, where they form an abrupt pointy lateral expansion which narrows again to form the olfactory tract.

Laterally to the olfactory region and in front of the orbits, the posterior region of the left nasolacrimal duct has been preserved (orange color in Figures 7b,d and 8b). It consists of a trilobed structure that joins in a single cavity anteriorly. Posteriorly it bifurcates into two ducts that connect with the anterior margin of the orbit. The medial duct is much larger and opens into a large lacrimal foramen at the anterior orbital margin. The lateral duct is smaller and opens into a tiny foramen at the anterolateral margin of the orbit.

Additionally, the posterior-most alveolar region has been preserved (Figures 7 and 8). This region is supplied by numerous blood vessels, but only the posterior end of the dorsal alveolar canal has been preserved. This canal houses the maxillary branches of the trigeminal nerve and several maxillary veins and arteries.

Posteroventrally to the olfactory region of the nasal cavity, the nasopharyngeal ducts have been preserved (light yellow color in Figures 7 and 8). In its route, they are enclosed by the palatines in its most anterior region and by the pterygoids in its posterior end. In its anterior-most preserved region these ducts are separated and run anteroposteriorly (Figure 7c,d). Posteriorly, they approach medially until they come into contact at the mid-length of the palatines and just posteriorly to the olfactory region (Figure 7c,d). Therefore, both ducts unify in a single large cavity, but they still preserve a small recess of the septum in its dorsal and ventral walls visible by the presence of sagittal grooves in the cavity (Figure 7c,d). In ventral view, when it passes through the posterior-most region of the palatines, the ventral wall of the duct narrows, forming a medial constriction, from which it widens again posteriorly (Figure 7d). This constriction is not visible in dorsal view since the dorsal and lateral walls of the canal maintain a constant width. At approximately the level of this constriction, the dorsal septum recess and its associated sagittal groove disappear, in consequence, the dorsal wall of the duct remains smooth. The ventral sulcus remains until the posterior end of the duct. When the nasopharyngeal duct passes through the pterygoids, it slopes slightly posteroventrally and continues in this direction until it opens through the internal choana (Figure 8a–d). In the

region of the pterygoids, the cross-section of the duct changes being wider ventrally than dorsally and having an inverted heart-shaped outline.

3.3.2 | Brain

The entire brain is complete and well-preserved (blue color in Figures 7–9). In dorsal view, it shows a slender and elongated overall morphology. In lateral view, the brain presents the typical sigmoidal or S-shaped outline observed in all mesoeucrocodylians (Bona et al., 2013, 2017; Kley et al., 2010; Serrano-Martínez et al., 2019a, 2021). The degree of their sigmoidal shape varies depending on the flexion angles between the forebrain–midbrain (cephalic flexion, CF) and the midbrain–hindbrain (pontine flexion, PF) (Figure 9f). This flexure varies from straighter and more tubular brains (high CF and PF values), as in thalattosuchians such as *Plagiophtalmosuchus*, *Macrospandylus*, *Cricosaurus*, *Pelagosaurus* and '*Metriorhynchus*', to more flexed sigmoidal brains (low CF and PF values), as in crocodylians such as *Alligator* (Erb & Turner, 2021; Pierce et al., 2017) or *Trilophosuchus* (Ristevski, 2022). The flexion values observed in *Portugalosuchus* are relatively high (CF = ~159°; PF = ~159°) indicating an intermediate brain morphology between *Plagiophtalmosuchus* (CF = 175°; PF = 170°), *Macrospandylus* (CF = 170°; PF = 165°), and *Gavialis* (CF = 150°; PF = 154°), falling in a similar range to that observed in *Pelagosaurus* (CF = 160°; PF = 160°) (Erb & Turner, 2021; Pierce et al., 2017). This greater angle in pontine flexion produces that the dorsal region of the cerebellum is approximately at the same height of the dorsal surface of the cerebrum in contrast with most nongavialoid crocodylians.

The olfactory bulbs are situated along the sagittal axis and bounded anteriorly and laterally by the olfactory region, posteriorly by the olfactory tract, and dorsally with the frontal bone between the orbits. They are two convex and parallel lobes, divided by a shallow longitudinal groove, that advance anteriorly until they taper in the olfactory region of the nasal cavity (Figure 7b). The bulbs appear to be unusually long compared with other crocodylomorphs; however, its anterior end is difficult to distinguish since the bulbs merge with the olfactory region without any visible structure marking the limit.

The olfactory tract is anteroposteriorly elongated, dorsoventrally flattened and maintains a constant lateromedial width until it reaches the area that joins the cerebrum in the prosencephalon (or forebrain) (Figure 9). As in most mesoeucrocodylians, the tract is undivided differing from the thalattosuchian *Pelagosaurus*, which shows two paired ducts in the anterior region of the tract (Pierce et al., 2017). At mid-length there is a small lateral deviation of the tract due to slight lateral shear deformation (Figure 9a,b). Posteriorly to this middle region, the tract progressively widens laterally until it contacts the cerebrum.

The prosencephalon is dorsally enclosed by the frontal and parietal, lateroventrally by the laterosphenoids and ventrally by the parabasisphenoid. The dorsal surface of the cerebrum is smooth,

relatively flat in its anterior region and becomes more rounded and convex posteriorly. In dorsal view, the posterior expansion of the cerebral hemispheres is so gradual that there is not a remarkably rounded convexity highlighting the anterior margin of the hemispheres (Figure 9a). This contrasts with the morphology of the cerebral hemispheres observed in most eusuchians, which tend to have rounded or conical dorsal outlines (Ristevski, 2022; Serrano-Martínez, 2019). On the contrary, the rounded morphology of the hemispheres in their posterior margin is more evident due to a more abrupt narrowing of the brain in the transition from the prosencephalon to the mesencephalon (or midbrain). The maximum width of the brain coincides with the lateral expansion of the cerebral hemispheres and its ratio with the greatest width of the hindbrain is about 1.15, which is similar to that observed in gavialoids such as *G. gangeticus* and *T. borissiakii* and different from most Crocodyloidea and Alligatoidea that usually present ratios between 1.5 and 2. In lateral view, the development of the cerebral hemispheres is also different from the morphology observed in most eusuchians. The hemispheres of *Portugalosuchus* have a more anteroposterior development, being slightly flattened dorsoventrally (Figure 9d,e), while in other eusuchians the hemispheres are more dorsoventrally expanded. This softness of the general contour seen in both dorsal and lateral views gives the brain of *Portugalosuchus* a more elongated appearance with less pronounced differences between the brain regions as contrast with other nongavialoid crocodylians.

The prosencephalon is posteroventrally bounded by the pituitary or hypophyseal fossa. The pituitary grows from the posteroventral margin of the forebrain as a straight and posteroventrally directed subcylindrical projection (Figure 9f). This morphology contrasts with the pituitary observed in some crocodylians such as *C. niloticus*, *A. mississippiensis*, *D. tormis* or allodaposuchids such as *Agaresuchus* and *Arenysuchus*, whose pituitary forms a curved elbow that begins ventrally directed to ends up bending posteriorly (Puértolas-Pascual et al., 2022; Serrano-Martínez et al., 2021), or with the subhorizontal pituitary observed in some thalattosuchians (Ristevski, 2022). From the posterior end of the pituitary arise the two bifurcated cerebral carotid arteries. The arteries run posterolaterally, then curve posterodorsally, cross the pharyngotympanic sinus and turn posteroventrally to exit by the posterior carotid foramen into the otoccipital (Figure 9).

In lateral view, the dorsal transition between the prosencephalon and the mesencephalon is very subtle (Figure 9d–f). There is only a slight concavity, much more evident in dorsal view, in the region of the optic lobe. A similar morphology has been observed in taxa such as *G. gangeticus*, however, in most eusuchians, there is a downward slope as the dorsal surface of the midbrain is more ventrally located. Some taxa, such as alligatoroids, even have a marked lump anteriorly to the slope between both regions of the brain (Serrano-Martínez, 2019). Posteriorly to the neck formed by the optic lobe region, the mesencephalon contacts the rhombencephalon, which expands dorsoventrally until reaching the maximum dorsoventral thickness of the brain marked by convex areas in the dorsal (cerebellum) and ventral (beginning of the medulla) surfaces (Figure 9f).

Almost in the contact area with the rhombencephalon, the lateroventral region of the mesencephalon holds the trigeminal nerve V which will be explained in the next subsection.

The boundary between the mesencephalon and the rhombencephalon (or hindbrain) is marked by the posterior margin of the opening for the trigeminal nerve V and the anterior margin of the concavities of the otic capsules (Figure 9). In dorsal view, this area of the rhombencephalon is characterized by strong dorsolateral constrictions of the brain, forming two large concavities that house the otic capsules and the inner ear (Figure 9a). Posteriorly to the otic capsules, the dorsal region of the hindbrain expands laterally again until it exits through the foramen magnum. Just before this exit, there is a small sagittal ridge on the dorsal surface associated with two lateral small depressions (Figure 9a). The ventral surface of the posterior-most region of the hindbrain is crossed by a sagittal ridge that may correspond to endocranial vasculature, most likely the basilar artery (see Porter et al., 2016: Figure 5) (Figure 9b). In lateral view, posteriorly to the large dorsoventral expansion of the cerebellum and pons regions, the hindbrain progressively reduces its dorsoventral thickness towards the medulla (Figure 9d–f). Posteriorly to the otic capsules, the hindbrain gets a constant thickness until its posterior end (Figure 9d,e).

3.3.3 | Cranial nerves

Due to its exceptional preservation, most of the nerves could be reconstructed (yellow color in Figures 7–9). The optic (II), oculomotor (III), trochlear (IV), trigeminal (V), abducens (VI), facial (VII), glossopharyngeal (IX), vagus (X), accessory (XI) and the paired canals of the hypoglossal nerves (XII) have been preserved. The olfactory (I) nerves could not be reconstructed by CT scan since they are located in the anteroventral region of the olfactory bulbs and, therefore, not enclosed within bony cavities. The vestibulocochlear (VIII) nerve can barely be distinguished or segmented; however, two to three small foramina in the prootic adjacent to the endosseous labyrinth can be observed (Figure 4c). This difficulty in distinguishing this nerve is common in larger specimens, where the growth of the inner ear and its approach to the nerve make its distinction more difficult (Lessner & Holliday, 2022). The accessory (XI) nerve cannot be reconstructed as it develops outside of the skull.

The optic (II) nerve, which serves to transmit visual sensory signals, has been preserved. It is a short, thick nerve located in the anteroventral region of the telencephalon, around the sagittal plane (Figure 9b,d,e). It extends anteriorly, outside the endocranial cavity; therefore, it has only been possible to reconstruct the most posterior end attached to the forebrain.

Both left and right oculomotor (III) nerves, which transmit motor signals, have been preserved. They are anteroposteriorly elongated nerves located anterolaterally to the pituitary fossa (Figure 9b,d,e). This nerve is laterally bounded by the laterosphenoid and its anterior exit is placed laterodorsally to the parabasisphenoid rostrum. However, the preserved cavity for this nerve does not completely

correspond to CN III as large vessels path through these foramina, as opposed to the canals of other cranial nerves (see models by Lessner & Holliday, 2022).

Left and right trochlear (IV) nerves have been preserved (Figure 9b,e). This nerve is responsible for transmitting motor sensory signals. The preserved cavity corresponds to a short path just below the cerebral hemisphere. In addition, most of the course of the right nerve merges with the cavity of the ophthalmic division (V_1) of the trigeminal nerve, and the exact limits between both nerves are difficult to distinguish (Figure 9d).

Both trigeminal (V) nerves are well-preserved (Figure 9a–e). As in other archosaurs, the trigeminal is the largest of the cranial nerves and transmits both motor and sensory signals. This nerve is divided into three main divisions (ophthalmic division V_1 , maxillary division V_2 and mandibular division V_3), as well as several subdivisions and secondary branches such as the supraorbital branch (nSO) and the tympanic branch (nTYM). In ML1818 most of the main divisions and some secondary branches can be reconstructed and, when it is not possible, their paths can be inferred thanks to the presence of grooves and bridges in the braincase. A trigeminal foramen surrounded by grooves identified as channels for the trigeminal nerve has already been described in several crocodylomorphs (Brochu et al., 2002; Holliday & Witmer, 2009). The shape and presence of these grooves, laterosphenoid bridges and epipterygoid vary among Crocodylomorpha (see Holliday & Witmer, 2009 for a more comprehensive explanation and distribution of these structures).

The trigeminal (V) nerve is a structure that flares from the lateral region of the mesencephalon until it exits through the big and sub-circular trigeminal foramen bounded by the prootic, laterosphenoid, quadrate and pterygoid. Most of the ophthalmic division (V_1) has been preserved in both sides of the skull (Figure 9d,e). This division exits through the trigeminal foramen and runs anteriorly from the main trigeminal trunk (trigeminal ganglion) through an anteroposterior groove in the lateral wall of the laterosphenoid (Figures 5a,b and 9b,d,e). This groove is open laterally (rather than being a closed tunnel); therefore, the laterosphenoid lacks a complete lateral bridge (Figure 5a,b). The beginning of the maxillary division (V_2) follows a similar direction almost parallel to V_1 (Figure 9d). However, V_2 starts slightly more dorsal than V_1 and runs slightly more anterolaterally rather than anteriorly (Figure 9a). As a consequence of its more anterolateral trajectory, only the beginning of the V_2 branch leaves some imprint on the lateral wall of the laterosphenoid (Figures 5a,b and 9d). The mandibular division (V_3) is projected ventrolaterally from the main trigeminal trunk and the trigeminal foramen, in consequence, it is not touching the bone surface in its path and there is almost not visible mark on the braincase wall (Figures 5a,b and 9d). On the left side, there is a groove that starts from the trigeminal foramen and runs dorsally through the medial wall surface of the supratemporal fossa, approximately between the laterosphenoid and the quadrate suture. This groove (g nSO, supraorbital nerve groove) holds the supraorbital branch (nSO) of nerve V and, on the right side of the skull, it passes under the caudal bridge of the laterosphenoid (Figures 5a,b and 9a,d) as in most extant taxa (Holliday &

Witmer, 2009). On the contrary, this bridge appears to be eroded on the right side and only a groove can be observed. Another two secondary dorsal branches can be observed in ML1818. The longest one corresponds to the tympanic branch (nTYM) of the trigeminal nerve (Figure 9a–e). The nTYM is completely enclosed within the braincase wall and it is a nearly straight posterolaterally directed branch, which takes off from the posterodorsal region of the main trigeminal trunk, passes through a foramen in the prootic and ends merging between the cavities of the pharyngotympanic sinus and the intertympanic diverticula. The shorter dorsal branch (nDO) begins in the dorsomedial region of the main trigeminal trunk, close to the beginning of the tympanic branch but in the opposite sense (Figure 9a,d,e). It curves dorsomedially until it connects with the dorsolateral surface of the mesencephalon where the optic lobe is located. The function of this dorsal branch remains unclear since it even could be a vascular blood vessel rather than a nerve branch.

On both sides, the abducens nerves (VI) are very thin canals originating from the ventrolateral surface of the mesencephalon region (Figure 9b,d). These nerves, linked with motor signals, are usually very thin and hard to recognize by CT scan (Serrano-Martínez, 2019), but they are clearly visible in *Portugalosuchus*. From the medulla, they run anteriorly along ventrally curved canals until they reach both sides of the pituitary where upon they exit the skull.

Both left and right cranial (VII) nerves, responsible for transmitting motor and sensory signals, have been reconstructed (Figure 9b–e). This nerve begins at the anteroventral margin of the otic capsule, just posterior to the trigeminal root. It bifurcates in the dorsal hyomandibular branch entering into the cavity of the pharyngotympanic sinus, and the ventral palatal branch, which enters within the cavity of the parabasisphenoid diverticulum (pneumatic recess). Ventrally, it passes through the latter cavity and cannot be distinguished in the CT scan; however, it exits again through the ventromedial wall of the parabasisphenoid diverticulum. From this exit, this nerve turns anteriorly and becomes elongated, anteroposteriorly oriented and runs parallel and close to the sagittal axis below the pituitary fossa. In its preserved anterior region, the nerve crosses the parabasisphenoid and exits through a small foramen between the pterygoid and the parabasisphenoid located ventrolaterally to the beginning of the parabasisphenoid rostrum (Figure 6c).

The glossopharyngeal (IX) and vagus (X) nerves have been preserved, but are only complete on the right side (Figure 9a–d). These nerves, which transmit both motor and sensory signals, are posterolaterally directed and posteriorly located to the inner ear, on the lateral margin of the hindbrain. The glossopharyngeal (IX) is a short nerve located close to the brain and ventrally to the vagus nerve (X). Both nerves merge in the common canal for CN IX, X, and sympathetic nerve, from where they open through the foramen vagi (or jugular foramen) on the posterior side of the otoccipital, dorsal to the foramen caroticum and anterolateral to the hypoglossal foramina (CN XII) (Figures 2f, 5j and 9a–e). At the midpoint of the common canal for CN IX, X, and sympathetic nerve, the tympanic branch of the vagus nerve (Xtym) splits from the rest and runs anterolaterally until it merges with the pharyngotympanic sinus. However, recently,

Kuzmin et al. (2021) argued that the tympanic branches of CN IX and X proposed by Lessner and Holliday (2022) may actually correspond to the sympathetic nerve that extends in a similar direction, enters the braincase via foramen vagi in the otoccipital and exits it anteriorly via the foramen within the prootic (see Neurocranial osteology above). The accessory (XI) nerve would be located outside this foramen so it cannot be reconstructed.

The hypoglossal (XII) are short, paired nerves which transmit motor signals. The pair of nerves on the right side are complete, while on the left side only the most anterior canal has been preserved (Figure 9a–e). This left anterior canal is bifurcated into two smaller ducts, something that is not seen on the right side. The hypoglossal nerve passes through two canals starting from the medulla, in the hindbrain lateral surface, and extending laterally until the hypoglossal foramina opening on the otoccipital (Figures 2f and 5j). Both nerves run parallel (also parallel to the vagus nerve), starting laterally and curving slightly posterolaterally from the midpoint toward their exit close to the foramen magnum. The posterior canal of the hypoglossal nerve is slightly wider and its opening foramen is more dorsally located than in the anterior canal.

3.3.4 | Paratympanic sinus system

In ML1818, the pharyngotympanic and median pharyngeal sinus systems are complete and well-preserved, and just the posterior region of the left pharyngotympanic sinus has been lost (Figures 7 and 8). These systems are housed in bony recesses around the hindbrain and slightly around the midbrain.

The pharyngotympanic system (green color in Figures 7 and 8) is the principal and biggest pneumatic complex of the paratympanic sinus system and extends laterally from the inner ear until it reaches the opening of the external auditory meatus. In this opening, the pharyngotympanic sinus expands anteroposteriorly. This expansion is much longer in posterior direction since it coincides with the cranioquadrate passage located between the paroccipital process of the otoccipital and the quadrate. Unfortunately, whether this passage is laterally open (as in hylaeochampsids and allodaposuchids), or laterally closed by the squamosal (as in crocodylians), cannot be determined in *Portugalosuchus* as this area is eroded. It should be noted that the cranioquadrate passage is not part of the paratympanic sinus system, since it serves as a neurovascular passage for nerves (CN VII) and blood vessels (stapedial vein and artery), and it is delimited from the paratympanic cavities by soft tissue not preserved in fossils (Kuzmin et al., 2021; Montefeltro et al., 2016). The right siphonium has been preserved, just the distal region and its exit through the foramen aereum are not preserved, as the distal region of the quadrate is eroded. The siphonium is a cylindrical canal that crosses the quadrate in a posterolateral direction. In its beginning, after starting from the posteroventral margin of the lateral pharyngotympanic sinus, the siphonium has a short anterior projection that corresponds to the quadrate recess. In the dorsolateral region of each pharyngotympanic sinus, close to the external auditory meatus, this cavity sends

a thin, cylindrical temporal canal over the dorsolateral surface of the lateral region of the intertympanic diverticulum. This canal exits anteriorly through the anterior temporal foramen, which is located in the posterior wall of the supratemporal fossa and surrounded by the squamosal, the parietal and the quadrate. More medially, this canal has another exit through the post-temporal fenestra, an opening located in the occipital region of the skull and surrounded by the supraoccipital, parietal and squamosal. It should be emphasized that the temporal canal is not a structure directly related to hearing and the paratympanic sinus system, since it serves as a passage for the main branches of the temporo-orbital artery and vein (Kuzmin et al., 2021; Porter et al., 2016; Walker, 1990). Ventromedially, the pharyngotympanic sinus extends surrounding the carotid artery and spreading under the brain. In this region and near the sagittal plane, the floor of both pharyngotympanic sinuses (the rhomboidal recess) extends ventromedially forming the basioccipital recess, two symmetric slender cavities that reach the medial pharyngeal sinus forming a Y-shaped connection. Laterally to these ventromedial cavities, the pharyngotympanic sinuses connect with the pharynx by the pharyngotympanic tubes. They are long and very thin ducts that run ventrally within the otoccipital, basioccipital and parabasisphenoid. The right pharyngotympanic tube is complete, and, near its distal end, it curves slightly posteroventrally until it exits through the lateral pharyngotympanic (= Eustachian) foramina at the same level with the median pharyngeal foramen such as in several species of *Crocodylus* (Brochu, 1999; Kuzmin et al., 2021). Unlike other observed crocodylians, the distal end of the pharyngotympanic canal and its foramen are located exclusively within the parabasisphenoid, without contact with the basioccipital. Interestingly, some recesses of the paratympanic sinus system that appear in many crocodylians, such as the pterygoid, the infundibular, the laterosphenoid and the prootic recesses, are absent in *Portugalosuchus*, presenting a similar condition to *G. gangeticus*, *T. schlegelii* and several crocodylids, where these recesses are greatly reduced or absent (Kuzmin et al., 2021).

The median pharyngeal (= Eustachian) canal (purple color in Figures 7 and 8) lies in the sagittal plane, and it is a long, thick, cylindrical tube slightly flattened dorsoventrally. This duct runs posteroventrally until it exits through the median pharyngeal foramen between the parabasisphenoid and the basioccipital. There is a slight sagittal ridge on its posterodorsal surface. At its dorsal end, the median pharyngeal canal forks to contact the pharyngotympanic sinuses dorsally and the parabasisphenoid diverticula anterodorsally. The contact with the parabasisphenoid diverticula (violet color in Figures 7 and 8) is also Y-shaped. Both diverticula have a small, rounded ventral expansion just after their dorsal bifurcation. From this point, they extend dorsally to contact the anterior ventromedial region of the pharyngotympanic sinuses.

The intertympanic diverticula (sky blue color in Figures 7 and 8) are complete and well-preserved. These cavities are dorsally located to the brain and the pharyngotympanic sinuses, and housed by the supraoccipital, otoccipitals and prootics. This pneumatic complex can be divided into three main regions: two lateral cavities and a central one. The central region, located within the supraoccipital, is

small and laterally connected to the lateral regions. These connections are produced by two cylindrical cavities which are almost as wide as the central region, which is greatly reduced in comparison with the lateral ones. In dorsal view, the central region together with these pillars form an anteriorly concave cavity. The lateral regions of the intertympanic diverticula are large rounded and ellipsoidal cavities housed within the prootics and the otoccipitals that extend laterally over almost the entire surface of the pharyngotympanic cavities. On the posteromedial surface of each lateral region, near the inner ear, the intertympanic diverticulum has a ventral projection. Several basal eusuchians, such as *Lohuecosuchus*, and most crocodylians, have a parietal diverticulum that emerges anteromedially from both lateral regions of the intertympanic diverticula. This structure consists of two prongs that approach each other medially or even converge to form a ring (Serrano-Martínez, 2019). However, there is no trace of any kind of parietal diverticulum in *Portugalosuchus*, having this anterior region quite smooth.

3.3.5 | Inner ear

In ML1818, both inner ears (light pink color in Figures 9 and 10) are well-preserved and almost complete. The inner ears are housed into two concavities located on the lateral sides of the rhombencephalon, specifically in the anterior region of the metencephalon, which form the otic capsules within the prootics and the otoccipitals. The inner ear is composed by the bony labyrinth system, which is a series of interconnected ring-shaped canals housing neurosensory organs related to balance, the vestibule, also related to balance, and the cochlear region containing the hearing organs. Both left and right bony labyrinths are well-preserved in ML1818, with semicircular canals without signs of deformation. The anterior semicircular canal is the longest and highest, although its duct diameter is slightly thinner than in the other canals. In lateral view, the anterior canal ascends anterodorsally from the wide and short crus commune until reaching the highest point of the inner ear, from where it descends abruptly anteroventrally until it contacts the vestibule and the lateral (or horizontal) semicircular canal. This area of contact between the canals and the vestibule, called anterior ampula, is anteriorly projected from the main body of the inner ear. The posterior canal has a similar morphology to the anterior one but in the opposite direction, slightly ascending posterodorsally from the crus commune and descending posteroventrally until it contacts the lateral canal in the posterior region of the inner ear. In this contact region between canals, there is also a posterior projection of the posterior ampula, although less pronounced than the anterior ampula. The diameter of the ring formed by the posterior canal is smaller, although the diameter of its duct is slightly larger than that of the anterior canal. In dorsal view, the angles formed between the planes of the anterior and the posterior canals are about 65°. The lateral canal is located laterally to the vestibule and forms a ring whose plane is horizontal. This canal is the shortest and forms the ring with the smallest

diameter of the three canals, although the diameter of the duct is slightly larger and slightly dorsoventrally flatter. In lateral view, the angle formed by the lateral and the anterior canals is about 69° in the left inner ear and 67° in the right one. The angle between the lateral and the posterior canals is about 50° in the left inner ear and 65° in the right one. The cochlear ducts (lagena) of both inner ears are ventrally projected, although in the right, which is better-preserved, a slight posterior deviation can be observed in its ventral end.

3.4 | Estimation of neurosensorial capabilities

The obtained 3D meshes can be also used to estimate some of the sensorial and cognitive capabilities of *Portugalosuchus*, by taking and comparing linear and volumetric measurements from concrete regions of the reconstructed inner skull cavities (see Supplementary Information S1 for tables with all measurements).

Olfactive acuity seems to be related to the number and size of the olfactory receptor genes, odor receptors and mitral cells (Zelenitsky et al., 2009), which are correlated with the absolute and relative size of the olfactory bulbs (Lautenschlager et al., 2012; Zelenitsky et al., 2009). Olfactory ratios were estimated by comparing the greatest diameter of the olfactory bulb with that of the brain hemisphere, normalized by a log transformation (Zelenitsky et al., 2009, 2011). The olfactory ratio of *Portugalosuchus* is 1.64 (Supplementary Information S1: Table S1), a bit low for a eusuchian (Puértolas-Pascual et al., 2022; Serrano-Martínez et al., 2019a, 2021).

Hearing acuity in reptiles and birds seems to be related to the size of the Endosseous Cochlear Duct (ECD), in the cochlear region (Walsh et al., 2009). The ECD of *Portugalosuchus* was measured, scaled to basicranium length and finally log transformed. The obtained result, -0.91 (Supplementary Information S1: Table S2), is within the range of crocodylians described by Walsh et al. (2009), and close to that of those estimated for other large eusuchians such as *Alligator mississippiensis*, *Crocodylus niloticus* or the extinct *Lohuecosuchus megadontos* (Serrano-Martínez, 2019).

There is no method to measure the size of the real eyeball in fossil crocodylomorphs, the organs used to estimate visual acuity (Hall & Ross, 2007; Lautenschlager et al., 2012; Schmitz, 2009). However, the relative volume of the optic lobes can be tested by comparing the volume of the optic lobes to that of the whole endocast volume (Jirak & Janacek, 2017, Figure 2; Serrano-Martínez et al., 2019a, 2021; Watanabe et al., 2019). The relative volume of the *Portugalosuchus* optic lobe is about 10% (Supplementary Information S1: Table S3), being close to that of *Tomistoma* and *Arenysuchus* (Puértolas-Pascual et al., 2022).

Finally, its cognitive capabilities can be estimated by calculating the reptile encephalization quotient (REQ; Hurlburt, 1996), an equation that compares the body mass (estimated based on skull measurements: Dodson, 1975; Platt et al., 2011; Webb & Messel, 1978)

and brain mass applying a density of 1 g/cm³ (Franzosa, 2004) to the brain volume. Brain volume was estimated after subtracting the volume of the dural envelope basing on a linear regression (Jirak & Janacek, 2017; Watanabe et al., 2019). The estimated REQ of *Portugalosuchus* is 0.97 (Supplementary Information S1: Table S4), within the range of other large-sized eusuchians, such as *A. mississippiensis*, *C. niloticus*, *T. schlegelii*, or the extinct *Agaresuchus fontisensis* (Serrano-Martínez et al., 2021).

3.5 | Neurosensorial implications

There are several studies about the acute sense of olfaction of crocodylians, having large olfactory bulbs in comparison with other archosaurs (Grigg & Kirshner, 2015; Zelenitsky et al., 2009, 2011). Based on the scarce available data, crocodylians have a slightly higher olfactory sense than alligatoroids, and basal eusuchians were located between both groups (Serrano-Martínez et al., 2019a, 2021). However, based on the latest studies (Puértolas-Pascual et al., 2022), allodaposuchids seem to have a lower average olfactory ratio than previously described, being more likely close to gavialoids and alligatoroids than to crocodylians. In this context, *Portugalosuchus* shows a lower olfactory ratio than that observed in other eusuchians and is closer to that observed in some allodaposuchids such as *Ar. gascabadiolorum* and *Ag. subjuniperus*, and the gavialoid *G. gangeticus*. In this way, the primitive condition would be to have "low" olfactory ratio, and crocodylians and tomistomines might have derived to a higher olfactory acuity.

Concerning audition, crocodylians seem to have a hearing acuity specialized towards low frequencies (Brusatte et al., 2016; Pierce et al., 2017; Vergne et al., 2009; Walsh et al., 2009), and *Portugalosuchus* is not an exception. However, its observed range is closer to the medium-sized crocodylians, such as *Osteolaemus tetraspis* and *Caiman crocodilus*, than to the large-sized samples, such as the allodaposuchid *L. megadontos*, the crocodyloid *C. niloticus*, the gavialoid *G. gangeticus*, or the crocodyloid *C. niloticus* (Serrano-Martínez et al., 2019b).

Vision is also a very acute sense in crocodylians, having relatively complex eyes (Garrick & Lang, 1977; Nagloo et al., 2016). However, the sight in these animals seems to be related to the photic condition of their habitat rather than to other variables, such as prey selection (Nagloo et al., 2016; Serrano-Martínez et al., 2021). The relative size of the optic lobe of *Portugalosuchus* is at the lower part but within the range observed for allodaposuchids and crocodylians (Puértolas-Pascual et al., 2022; Serrano-Martínez et al., 2021). This may be due to an adaptation to more muddy waters like *Arenysuchus* and *Tomistoma schlegelii*.

Finally, the estimated REQ of *Portugalosuchus* (0.97) is quite similar to that of *A. mississippiensis*, *C. niloticus* (both REQs = 0.96) or *T. schlegelii* (REQ = 1.03), all of them large-sized specimens (Serrano-Martínez et al., 2021). This result agrees with the latest proposals, noticing that the REQ in crocodiles is closely related to the sample size (Serrano-Martínez et al., 2019a, 2021).

3.6 | Phylogenetic analysis

Thanks to the information obtained from the micro-CT scan several characters used in the original description of *Portugalosuchus azenhae* (ML1818) by Mateus et al. (2019) have been modified and new ones have been codified (see Supplementary Information S1 for the list of modified characters). In that work, ML1818 was included in the matrix of Narváez et al. (2016), matrix in turn based on the work of Brochu and Storrs (2012) among others, but all of them mostly based on the dataset of Brochu (1997b). However, recently Rio and Mannion (2021) published a new dataset that includes 330 characters (using continuous and discrete characters) and 144 taxa, being one of the most complete matrices for deeply nested neosuchian crocodylomorphs. These authors made an exhaustive description of each character including very comprehensive photos that help to better understand its meaning and reduce subjectivity and ambiguity during encoding. In addition, this dataset seems to solve the long-standing gharial problem by using exclusively morphological characters, obtaining similar results to DNA phylogenies and some recent DNA + morphological characters phylogenies (see Rio & Mannion, 2021 and references therein for a comprehensive

review of previous phylogenetic studies). For all these reasons we have decided to use the Rio and Mannion (2021) dataset and include the new *Portugalosuchus azenhae* coding there (see Supplementary Information S2 to get the matrix in .tnt format).

In the work of Rio and Mannion (2021) they carry out up to 9 different phylogenetic analyses (1.1 to 3.3) in which they change different parameters such as the use of continuous and/or discrete characters, the weighting, and the number of characters among others. From their work they conclude that the analysis that recovered the most stratigraphically congruent topology is 1.3 (Rio & Mannion, 2021: Figure 10) and for this reason we have used that protocol for our analysis. The analysis was performed using the New Technology Search in TNT v 1.5 (July 2022 version) (Goloboff & Catalano, 2016), with all algorithms enabled (Sect. search, Ratchet, Drift and Tree fusing) and the consensus tree stabilized 5 times with a factor of 75, leaving the rest of the options by default. To recover all trees, a second search using the trees recovered from the first New Technology Search iteration were used as starting trees for a traditional search (“trees from ram” option) using tree bisection and reconnection (TBR). The analysis was performed with the implied weighting and extended implied weighting activated using a $k = 12$

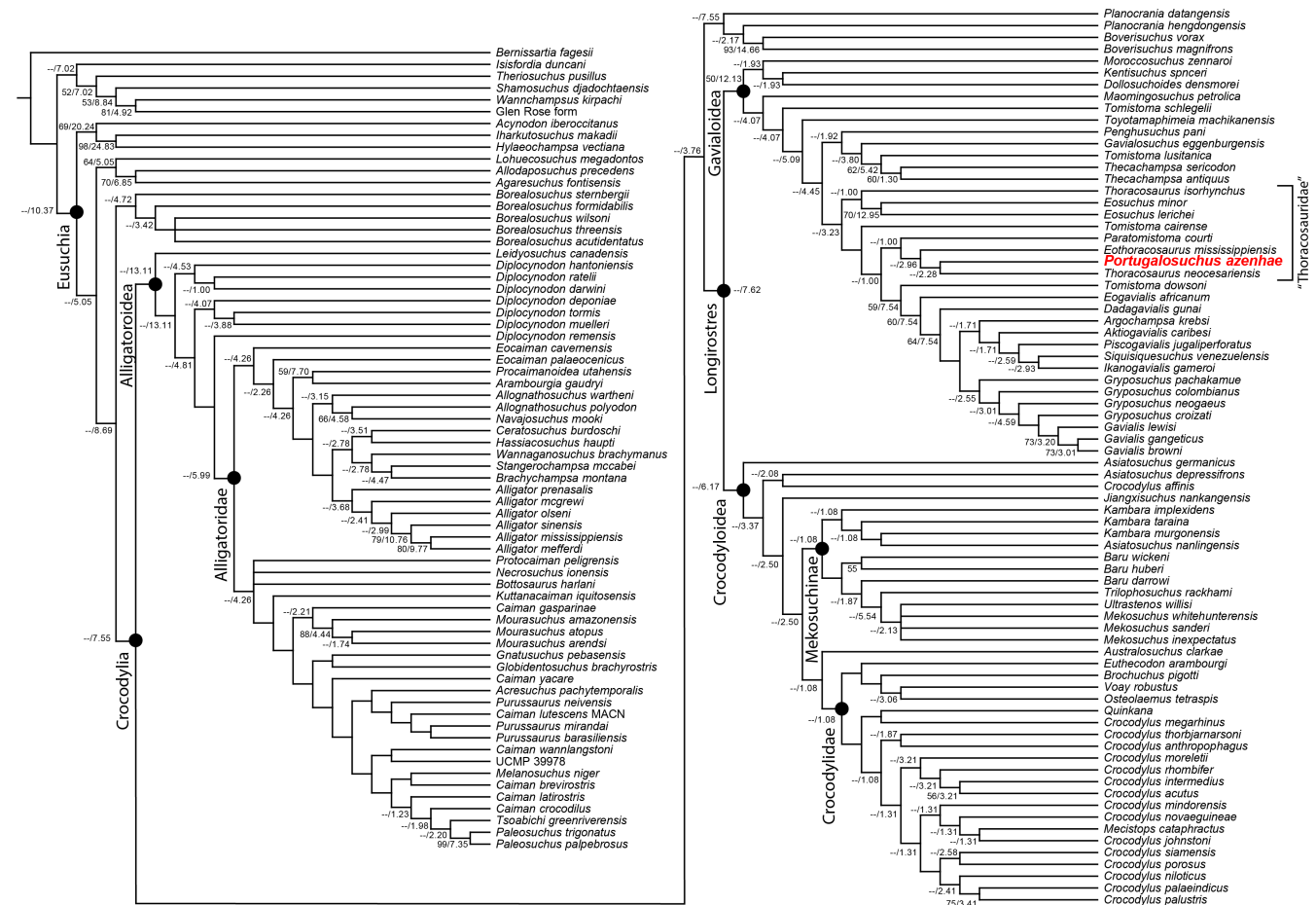


FIGURE 11 Phylogenetic relationships of eusuchians, depicting the position of *Portugalosuchus azenhae* (ML1818) based on the matrix of Rio and Mannion (2021). Strict consensus tree of 9 most parsimonious cladograms with 8199 of character fit score. Numbers of each node indicate the bootstrap frequencies over 50% and Bremer support over 1.

of weighting function in the basic settings and activating the “down-weight chars. with missing entries faster” option in the extended weighting menu (see Rio & Mannion, 2021 for a more detailed explanation of the use of extended implied weighting). Following this protocol, in our analysis 36 multistate characters were treated as ordered (characters 17, 37, 47, 48, 58, 65, 72, 75, 78, 81, 87, 88, 102, 109, 110, 137, 142, 151, 162, 175, 181, 188, 210, 214, 220, 221, 222, 224, 235, 243, 284, 293, 297, 308, 323, and 324). We have to highlight a small error in the TNT file of the supplementary information of the work of Rio and Mannion (2021), while in their article and in their description of characters they count characters 37, 110 and 220 as ordered, in the file TNT these characters appeared as unordered. We fixed this mistake in our analysis and found that it did not affect too much the original topologies obtained by Rio and Mannion (2021).

The search returned 9 most parsimonious trees (MPTs) with 8199 of character fit score (ensemble consistency index, CI = 0.178; ensemble retention index, RI = 0.654; rescaled consistency index, RC = 0.116). The bootstrap frequencies over 50% and Bremer support over 1 were summarized in the strict consensus tree (Figure 11).

The tree topology places *Portugalosuchus* within Crocodylia, as in the original phylogeny (Mateus et al., 2019; Figure 11). Nevertheless, it shows a different position within the crown group, and now it is recovered as a “thoracosaurid”, as in Rio and Mannion (Rio & Mannion, 2021; Figure 10). The distribution of the “thoracosaurids” is also slightly different from that shown in analysis 1.3 of Rio and Mannion (2021), since although our cladogram also recovers “Thoracosauridae” as paraphyletic, the taxa are divided into two successive clades with the taxon *Tomistoma cairensis* Müller, 1927 situated between them. *Portugalosuchus* appears within the most deeply nested clade of the “thoracosaurids” as the sister taxon of *Thoracosaurus neocesariensis* (de Kay, 1842) (Figure 11).

It is interesting to mention that the results obtained here and in the analysis by Rio and Mannion (2021) contrast slightly with other recent analyses that combine the use of DNA and morphological characters (Darlim et al., 2022; Lee & Yates, 2018). These aforementioned works place “Thoracosauridae” and *Portugalosuchus* (and other taxa such as *Borealosuchus* spp. and Planiocraniidae) outside of Crocodylia as successive sister eusuchian taxa of the crown group. It would be interesting to replicate these analyses including the new data obtained here, alongside DNA data, and using other cladistic approaches such as undated Bayesian and tip-dating Bayesian analyses, but a work so focused on phylogeny goes beyond the objectives of the present anatomical study.

4 | CONCLUSIONS

Since the turn of the twenty-first century, paleoneuroanatomy has advanced significantly as a result of CT technology. In this regard, here we show the results of the first detailed braincase anatomical description and neuroanatomical analysis of the holotype of the Portuguese Cenomanian eusuchian crocodylomorph *Portugalosuchus*

azenhae (ML1818). The resulting 3D model has allowed a detailed description of the neurocranium of ML1818, which has helped to correct and complete some of the observations of previous articles. It has also been possible to reconstruct the cavities of the olfactory region, nasopharyngeal ducts, brain, nerves, carotid arteries, blood vessels, paratympenic sinus system and inner ear.

Thanks to the reconstruction of the internal cavities, its neurosensorial capabilities were also estimated. The calculated olfactory acuity of *Portugalosuchus* is a bit low for Eusuchia, although not far from the range observed in this clade. Hearing acuity is very similar to that seen in medium-sized crocodylians. Visual acuity is also smaller than the eusuchian average, although it is within the range seen in allodaposuchids and crocodylians. Finally, the estimated REQ is quite similar to that of large-sized crocodylians such as *A. mississippiensis*, *C. niloticus*, or *T. schlegeli*. Therefore, these analyses show that back during the Cenomanian, *Portugalosuchus* already possessed olfactory acuity, sight, hearing, and cognitive abilities within the range observed in other basal eusuchians and crocodylians.

These new anatomical data were included in one of the most recent phylogenies based on morphological characters (Rio & Mannion, 2021). The position of *Portugalosuchus* differs slightly from the original publication (Mateus et al., 2019), as it is now placed as a thoracosaurid within Gavialoidea, but still within Crocodylia. This position contrasts with other recent analyses that include DNA information and that place *Portugalosuchus* outside of Crocodylia (Darlim et al., 2022). In order to adequately test these phylogenies, future cladistic analyses should take into account the new morphological traits seen in *Portugalosuchus* by encoding them alongside DNA data.

AUTHOR CONTRIBUTIONS

E.P.P., conceived and designed the study, collected the data, and wrote the manuscript; E.P.P., I.T.K. and A.S.M. wrote the paper, contributed data or analysis tools, and performed the analysis and interpretations; E.P.P., I.T.K., A.S.M. and O.M. reviewed the manuscript and approved the article; O.M. provided funding for the project.

ACKNOWLEDGMENTS

This research forms part of the project GeoBioTec UIDB/04035/2020, subsidized by the Fundação para a Ciência e a Tecnologia. E.P-P was supported by a postdoctoral grant funded by the Fundação para a Ciência e a Tecnologia, Portugal (SFRH/BPD/116759/2016), and by a postdoctoral contract (María Zambrano) funded by the Ministry of Universities of the Government of Spain through the Next Generation EU funds of the European Union. We want to acknowledge B. Notario (CENIEH) and Victor Beccari (SNSB – Bayerische Staatssammlung für Paläontologie und Geologie) for their help with the CT-scanning and the segmentation process. Thanks to the reviewers Jorgo Ristevski and Yanina Herrera for their helpful comments that greatly improved the manuscript.

DATA AVAILABILITY STATEMENT

The data that support the findings of this study are openly available at the Morphosource.org Digital Repository [ark:/87602/m4/494665; ark:/87602/m4/494670; ark:/87602/m4/494660]. The raw μ CT data for ML1818 is available upon request from the Museu da Lourinhã (Lourinhã, Portugal: <https://museoulourinha.org/>).

ORCID

Eduardo Puértolas-Pascual  <https://orcid.org/0000-0003-0759-7105>

Ivan T. Kuzmin  <https://orcid.org/0000-0003-3086-2237>

Alejandro Serrano-Martínez  <https://orcid.org/0000-0003-1178-6064>

Octávio Mateus  <https://orcid.org/0000-0003-1253-3616>

REFERENCES

- Bellairs, A. & Shute, C.C.D. (1953) Observations on the narial musculature of Crocodylia and its innervation from the sympathetic system. *Journal of Anatomy*, **87**, 367–378.
- Benton, M.J. & Clark, J.M. (1988) Archosaur phylogeny and the relationships of the Crocodylia. In: Benton, M.J. (Ed.) *The phylogeny and classification of the Tetrapods. Volume 1: amphibians, reptiles, birds*. Oxford: Clarendon Press, pp. 295–338.
- Blanco, A., Fortuny, J., Vicente, A., Luján, À.H., García-Marçà, J.A. & Sellés, A.G. (2015) A new species of *Allodaposuchus* (Eusuchia, Crocodylia) from the Maastrichtian (late cretaceous) of Spain: phylogenetic and paleobiological implications. *PeerJ*, **3**, e1171.
- Bona, P., Carabajal, A.P. & Gasparini, Z. (2017) Neuroanatomy of *Gryposuchus neogaeus* (Crocodylia, Gavialoidea): a first integral description of the braincase and endocranial morphological variation in extinct and extant gavialoids. *Earth and Environmental Science Transactions of the Royal Society of Edinburgh*, **106**, 235–246.
- Bona, P., Degrange, F.J. & Fernández, M.S. (2013) Skull anatomy of the bizarre Crocodylian *Mourasuchus nativus* (Alligatoridae, Caimaninae). *Anatomical Record*, **296**, 227–239.
- Brochu, C.A. (1997a) A review of 'Leidyosuchus' (Crocodyliformes, Eusuchia) from the cretaceous through Eocene of North America. *Journal of Vertebrate Paleontology*, **17**, 679–697.
- Brochu, C.A. (1997b) Morphology, fossils, divergence timing, and the phylogenetic relationships of *Gavialis*. *Systematic Biology*, **46**, 479–522.
- Brochu, C.A. (1999) Phylogenetics, taxonomy, and historical biogeography of Alligatoroidea. *Memoir of the Society of Vertebrate Paleontology*, **6**, 9–100.
- Brochu, C.A., Bouaré, M.L., Sissoko, F., Roberts, E.M. & O'Leary, M.A. (2002) A dyrosaurid crocodyliform braincase from Mali. *Journal of Paleontology*, **76**, 1060–1071.
- Brochu, C.A. & Gingerich, P.D. (2000) New tomistomine crocodylian from the middle Eocene (Bartonian) of Wadi Hitán, Fayum Province, Egypt. *Contributions from the Museum of Paleontology, University of Michigan*, **30**, 251–268.
- Brochu, C.A. & Storrs, G.W. (2012) A giant crocodile from the Pliocene of Kenya, the phylogenetic relationships of Neogene African crocodylines, and the antiquity of *Crocodylus* in Africa. *Journal of Vertebrate Paleontology*, **32**(3), 587–602.
- Brusatte, S.L., Muir, A., Young, M.T., Walsh, S., Steel, L. & Witmer, L.M. (2016) The braincase and neurosensory anatomy of an early Jurassic marine crocodylomorph: implications for crocodylian sinus evolution and sensory transitions. *The Anatomical Record*, **299**, 1511–1530.
- Buckley, G.A., Brochu, C.A., Krause, D.W. & Pol, D. (2000) A pug-nosed crocodyliform from the late cretaceous of Madagascar. *Nature*, **405**, 941–944.
- Buscalioni, A.D., Sanz, J.L. & Casanovas, M.L. (1992) A new species of the eusuchian crocodile *Diplocynodon* from the Eocene of Spain. *Neues Jahrbuch für Geologie und Paläontologie-Abhandlungen*, **187**, 1–29.
- Carvalho, I.D.S., Teixeira, V.P.A., Ferraz, M.L.F., Ribeiro, L.C.B., Martinelli, A.G., Neto, F.M. et al. (2011) *Campinasuchus dinizi* gen. Et sp. nov., a new late cretaceous baurusuchid (Crocodyliformes) from the Bauru Basin, Brazil. *Zootaxa*, **2871**, 19–42.
- Clark, J.M. & Norell, M.A. (1992) The early cretaceous crocodylomorph *Hylaeochampsia vectiana* from the Wealden of the Isle of Wight. *American Museum Novitates*, **3032**, 1–19.
- Colbert, E.H. (1946) The eustachian tubes in the Crocodylia. *Copeia*, **1946**, 12–14.
- Colbert, E.H., Simpson, G.G. & Williams, C.S. (1946) *Sebecus*, representative of a peculiar suborder of fossil Crocodylia from Patagonia. *Bulletin of the American Museum of Natural History*, **87**, 217–270.
- Cope, E.D. (1861) List of the recent species of Emydosaurian reptiles in the Museum of the Academy of natural sciences. *Proceedings of the Academy of Natural Sciences of Philadelphia*, **12**, 549–550.
- Cuvier, G.L. (1824) *Recherches Sur Les Ossements Fossiles*. Vol. 5. 2eme. Paris: G. Dufour & E. d'Ocagne Libraries, 185.
- Darlim, G., Lee, M.S., Walter, J. & Rabi, M. (2022) The impact of molecular data on the phylogenetic position of the putative oldest crown crocodylian and the age of the clade. *Biology Letters*, **18**(2), 20210603.
- Daudin, F.M. (1802) *Histoire Naturelle, Générale et Particulière des Reptiles. ouvrage faisant suit à l'Histoire naturell générale et particulière, composée par Leclerc de Buffon; et rédigée par C.S. Sonnini, membre de plusieurs sociétés savantes*, Vol. 2. Paris: F. Dufart, 432.
- de Kay, J.E. (1842) *Zoology of New York*. Albany: White & Visscher, 415.
- Dodson, P. (1975) Functional and ecological significance of relative growth in Alligator. *Journal of Zoology, London*, **175**, 315–355.
- Dufeu, D.L. & Witmer, L.M. (2015) Ontogeny of the middle-ear air-sinus system in *Alligator mississippiensis* (archosauria: Crocodylia). *PLoS One*, **10**, 1–25.
- Duméril, A. & Bibron, G. (1851) *Catalogue méthodique de la collection des reptiles*. Paris: Gide & Baudry, 224.
- Dumont, M.V., Jr., Santucci, R.M., de Andrade, M.B. & de Oliveira, C.E.M. (2022) Paleoneurology of *Baurusuchus* (Crocodyliformes: Baurusuchidae), ontogenetic variation, brain size, and sensorial implications. *The Anatomical Record*, **305**(10), 2670–2694.
- Edinger, T. (1938) Über Steinkerne von Hirn-und Ohr-Höhlen der Mesosuchier *Goniopholis* und *Pholidosaurus* aus dem Bückeburger Wealden. *Acta Zoologica*, **19**, 467–505.
- Efimov, M.B. (1975) Late cretaceous crocodiles of soviet Central Asia and Kazakhstan. *Paleontologicheskii Zhurnal*, **9**, 417–420.
- Erb, A. & Turner, A.H. (2021) Braincase anatomy of the Paleocene crocodyliform *Rhabdognathus* revealed through high resolution computed tomography. *PeerJ*, **9**, e11253.
- Fauvel, A.A. (1879) Alligators in China. *Journal of the North-China Branch of the Royal Asiatic Society, Shanghai New Series*, **13**, 1–36.
- Fernández, M. & Gasparini, Z. (2000) Salt glands in a Tithonian metriorhynchid crocodyliform and their physiological significance. *Lethaia*, **33**, 269–276.
- Fernández, M. & Gasparini, Z. (2008) Salt glands in the Jurassic metriorhynchid *Geosaurus*: implications for the evolution of osmoregulation in Mesozoic marine crocodyliforms. *Naturwissenschaften*, **95**, 79–84.
- Fernández, M.S., Carabajal, A.P., Gasparini, Z. & Díaz, G.C. (2011) A metriorhynchid crocodyliform braincase from northern Chile. *Journal of Vertebrate Paleontology*, **31**, 369–377.
- Fernández, M.S. & Herrera, Y. (2009) Paranasal sinus system of *Geosaurus araucanensis* and the homology of the antorbital fenestra of metriorhynchids (Thalattosuchia: Crocodylomorpha). *Journal of Vertebrate Paleontology*, **29**, 702–714.
- Fernández-Dumont, M.L., Bona, P., Barrios, F., Paulina Carabajal, P. & Apesteguía, S. (2017) Estudio preliminar del endocast de un ejemplar de *Araripesuchus* (Crocodyliformes, Uruguaysuchidae): aportes

- al conocimiento de la neuroanatomía de los notosuquios. *Reunión de Comunicaciones de la Asociación Paleontológica Argentina*, 32.
- Fonseca, P.H.M., Martinelli, A.G., Marinho, T.d.S., Ribeiro, L.C.B., Schultz, C.L. & Soares, M.B. (2020) Morphology of the endocranial cavities of *Campinasuchus dinizi* (Crocodyliformes: Baurusuchidae) from the upper cretaceous of Brazil. *Geobios*, 58, 1–16.
- Franzosa, J.W. (2004) *Evolution of the brain in Theropoda (Dinosauria)*. PhD Thesis. Austin: The University of Texas.
- Garrick, L.D. & Lang, J.W. (1977) Social signals and behaviours of adult alligators and crocodiles. *American Zoologist*, 17, 225–239.
- Gasparini, Z.B. (1985) Un nuevo cocodrilo (Eusuchia) Cenozoico de América del Sur. *Coletânea de Trabalhos Paleontológicos do IIX Congresso Brasileiro de Paleontologia, MME-DNPM*, 27, 51–53.
- Gervais, P. (1871) Remarques sur les reptiles provenant des calcaires lithographiques de Cerin. *Comptes Rendus Académie Sciences, Paris*, 73, 603–607.
- Gmelin, J.F. (1789) Regnum animale. In: Beer, G.E. & de la Mollière, A.J.B. (Eds.) *Caroli a Linné. Systema Naturae per regna tria naturae, secundum classes, ordines, genera, species; cum characteribus, differentiis, synonymis, locis* 1. Lyon, France: Leipzig, pp. 1033–1516.
- Goloboff, P.A. & Catalano, S.A. (2016) TNT version 1.5, including a full implementation of phylogenetic morphometrics. *Cladistics*, 32, 221–238.
- Grigg, G.C. & Kirshner, D. (2015) *Biology and evolution of Crocodylians*. Ithaca, New York: Cornell University Press, 650.
- Hall, M.I. & Ross, C.F. (2007) Eye shape and activity pattern in birds. *Journal of Zoology*, 271, 437–444.
- Hart, L.J., Bell, P.R., Smith, E.T. & Salisbury, S.W. (2019) *Isisfordia molnari* sp. nov., a new basal eusuchian from the mid-cretaceous of lightning ridge, Australia. *PeerJ*, 7, e7166.
- Hay, O.P. (1930) Second bibliography and catalogue of the fossil vertebrata of North America. *Carnegie Institute Wash Publications*, 390(2), 1–1074.
- Herrera, Y. (2015) Metriorhynchidae (Crocodylomorpha: Thalattosuchia) from upper Jurassic–lower cretaceous of Neuquén Basin (Argentina), with comments on the natural casts of the brain. *Publicación Electrónica de la Asociación Paleontológica Argentina*, 15(1), 159–171.
- Herrera, Y., Fernández, M.S. & Gasparini, Z. (2013) The snout of *Cricosaurus araucanensis*: a case study in novel anatomy of the nasal region of metriorhynchids. *Lethaia*, 46, 331–340.
- Herrera, Y., Leardi, J.M. & Fernández, M.S. (2018) Braincase and endocranial anatomy of two thalattosuchian crocodylomorphs and their relevance in understanding their adaptations to the marine environment. *PeerJ*, 6, e5686.
- Herrera, Y. & Vennari, V.V. (2015) Cranial anatomy and neuroanatomical features of a new specimen of Geosaurini (Crocodylomorpha: Metriorhynchidae) from west-Central Argentina. *Historical Biology*, 27, 33–41.
- Holliday, C.M. & Gardner, N.M. (2012) A new eusuchian crocodyliform with novel cranial integument and its significance for the origin and evolution of Crocodylia. *PLoS One*, 7, e30471.
- Holliday, C.M., Tsai, H.P., Skiljan, R.J., George, I.D. & Pathan, S. (2013) A 3D interactive model and atlas of the jaw musculature of *Alligator mississippiensis*. *PLoS One*, 8(6), e62806.
- Holliday, C.M. & Witmer, L.M. (2009) The epipterygoid of crocodyliforms and its significance for the evolution of the orbitotemporal region of eusuchians. *Journal of Vertebrate Paleontology*, 29, 715–733.
- Hopson, J.A. (1979) Paleoneurology. In: Gans, C., Northcutt, R.G. & Ulinski, P. (Eds.) *Biology of the reptilia, volume 9: neurology a*. New York: Academic Press, pp. 39–146.
- Hu, K., King, J.L., Romick, C.A., Dufeu, D.L., Witmer, L.M., Stubbs, T.L. et al. (2021) Ontogenetic endocranial shape change in alligators and ostriches and implications for the development of the non-avian dinosaur endocranium. *The Anatomical Record*, 304, 1759–1775.
- Hurlburt, G.R. (1996) *Relative brain size in recent and fossil amniotes: determination and interpretation*. [PhD Thesis]. Toronto, Canada: University of Toronto, 253.
- Huxley, T.H. (1875) On *Stagonolepis robertsoni*, and on the evolution of the Crocodilia. *Quarterly Journal of the Geological Society*, 31(1–4), 423–438.
- Iordansky, N.N. (1973) The skull of Crocodilia. In: Gans, C. & Parsons, T.S. (Eds.) *Biology of the reptilia, volume 4: morphology D*. New York: Academic Press, pp. 201–264.
- Jirak, D. & Janacek, J. (2017) Volume of the crocodylian brain and endocast during ontogeny. *PLoS One*, 12, e0178491.
- Jouve, S., Bardet, N., Jailil, N.-E., Suberbiola, X.P., Bouya, B. & Amaghaz, M. (2008) The oldest African crocodylian: phylogeny, paleobiogeography, and differential survivorship of marine reptiles through the cretaceous-tertiary boundary. *Journal of Vertebrate Paleontology*, 28, 409–421.
- Jouve, S., Bouya, B., Amaghaz, M. & Meslouh, S. (2015) *Maroccosuchus zennaroi* (Crocodylia: Tomistominae) from the Eocene of Morocco: phylogenetic and palaeobiogeographical implications of the basal-most tomistomine. *Journal of Systematic Palaeontology*, 13, 421–445.
- Kawabe, S., Shimokawa, T., Miki, H., Okamoto, T. & Matsuda, S. (2009) A simple and accurate method for estimating the brain volume of birds: possible application in paleoneurology. *Brain, Behavior and Evolution*, 74, 295–301.
- Kley, N.J., Sertich, J.J.W., Turner, A.H., Krause, D.W., O'Connor, P.M. & Georgi, J.A. (2010) Craniofacial morphology of *Simosuchus clarki* (Crocodyliformes: Notosuchia) from the late cretaceous of Madagascar. *Journal of Vertebrate Paleontology*, 30, 13–98.
- Konzhukova, E.D. (1954) New fossil crocodylians from Mongolia. *Trudy Paleontologicheskogo Instituta ANSSSR*, 48, 171–194.
- Krefftt, G. (1873) Remarks on Australian crocodiles, and description of a new species. *Proceedings of the Zoological Society of London*, 1873, 334–335.
- Kuzmin, I.T., Boitsova, E.A., Gombolevskiy, V.A., Mazur, E.V., Morozov, S.P., Sennikov, A.G. et al. (2021) Braincase anatomy of extant Crocodylia, with new insights into the development and evolution of the neurocranium in crocodylomorphs. *Journal of Anatomy*, 239, 983–1038.
- Kuzmin, I.T., Skutschas, P.P., Boitsova, E.A. & Sues, H.D. (2019) Revision of the large crocodyliform *Kansajsuchus* (Neosuchia) from the late cretaceous of Central Asia. *Zoological Journal of the Linnean Society*, 185(2), 335–387.
- Laurenti, J.N. (1768) *Specimen medicum, exhibens synopsis reptilium emendatum cum experimentis circa venena et antidota reptilium austriacorum*. Vienna: Joan. Thomae nob. de Trattner, 217.
- Lautenschlager, S., Rayfield, E.J., Altangerel, P., Zanno, L.E. & Witmer, L.M. (2012) The endocranial anatomy of therizinosauria and its implications for sensory and cognitive function. *PLoS One*, 7, e52289.
- Leardi, J.M., Pol, D. & Clark, J.M. (2017) Detailed anatomy of the braincase of *Macelognathus vagans* marsh, 1884 (Archosauria, Crocodylomorpha) using high resolution tomography and new insights on basal crocodylomorph phylogeny. *PeerJ*, 5, e2801.
- Leardi, J.M., Pol, D. & Clark, J.M. (2020) Braincase anatomy of *Almadasuchus figarii* (Archosauria, Crocodylomorpha) and a review of the cranial pneumaticity in the origins of Crocodylomorpha. *Journal of Anatomy*, 237, 48–73.
- Lee, M.S. & Yates, A.M. (2018) Tip-dating and homoplasy: reconciling the shallow molecular divergences of modern gharials with their long fossil record. *Proceedings of the Royal Society B*, 285(1881), 20181071.
- Lemoine, V. (1883) Note sur l'encéphale du gavial du Mont-Aimé, étudié sur trois moulages naturels. *Bulletin de la Société Géologique de France*, 3, 158–162.
- Lessner, E.J. (2021) Quantifying neurovascular canal branching patterns reveals a shared crocodylian arrangement. *Journal of Morphology*, 282, 185–204.

- Lessner, E.J. & Holliday, C.M. (2022) A 3D ontogenetic atlas of *Alligator mississippiensis* cranial nerves and their significance for comparative neurology of reptiles. *The Anatomical Record*, 305(10), 2854–2882.
- Linnaeus, C. (1758) *Systema naturæ per regna tria naturæ, secundum classes, ordines, genera, species, cum characteribus, differentiis, synonymis, locis*. Tomus I. Editio decima, reformata, 10th edition. Laurentii Salvii, Holmiæ, 824.
- Maria, F.C., Azevedo, S.A.K., de Carvalho, L.B., Henriques, D.D.R., do Amaral, R.V. & Rodrigues, I.F. (2010) Descrição da cavidade nasal, seios paranasais e seios timpânicos em *Mariliasuchus amarali* (Crocodyliformes, Notosuchia) do Neocretáceo brasileiro. *Boletim de Resumos do 7º Simpósio Brasileiro de Paleovertebrados*, 47.
- Martin, J.E., Smith, T., Salaviale, C., Adrien, J. & Delfino, M. (2020) Virtual reconstruction of the skull of *Bernissartia fagesii* and current understanding of the neosuchian–eusuchian transition. *Journal of Systematic Palaeontology*, 18, 1079–1101.
- Martinelli, A.G. & Pais, D.F. (2008) A new baurusuchid crocodyliform (Archosauria) from the late cretaceous of Patagonia (Argentina). *Comptes Rendus Palevol*, 7(6), 371–381.
- Mateus, O., Puértolas-Pascual, E. & Callapez, P.M. (2019) A new eusuchian crocodylomorph from the Cenomanian (late cretaceous) of Portugal reveals novel implications on the origin of Crocodylia. *Zoological Journal of the Linnean Society*, 186, 501–528.
- Melstrom, K.M., Turner, A.H. & Irmis, R.B. (2022) Reevaluation of the cranial osteology and phylogenetic position of the early crocodyliform *Eopneumatosuchus colberti*, with an emphasis on its endocranial anatomy. *The Anatomical Record*, 305(10), 2557–2582.
- Montefeltro, F.C., Andrade, D.V. & Larsson, H.C. (2016) The evolution of the meatal chamber in crocodyliforms. *Journal of Anatomy*, 228, 838–863.
- Mook, C.C. (1924) A new crocodylian from Mongolia. *American Museum Novitates*, 117, 1–5.
- Müller, L. (1927) Ergebnisse der Forschungsreisen Prof. E. Stromers in den Wüsten Agyptens. V. Tertiäre Wirbeltiere 1. Beiträge zur Kenntnis der Krokodilier des ägyptischen Tertiärs. *Abhandlungen der Bayerische Akademie der Wissenschaften. Mathematisch-Naturwissenschaftliche Abteilung*, 31(2), 1–96.
- Müller, S. (1838) Waarnemingen over de Indische Krokodillen en Beschrijving Van Enne Nieuwe Soort. *Tijdschrift voor Natuurlijke Geschiedenis en Physiologie, Amsterdam and Leyden*, 5, 61–87.
- Nagloo, N., Collin, S.P., Hemmi, J.M. & Hart, N.S. (2016) Spatial resolving power and spectral sensitivity of the saltwater crocodile, *Crocodylus porosus*, and the freshwater crocodile, *Crocodylus johnstoni*. *The Journal of Experimental Biology*, 219, 1394–1404.
- Narváez, I., Brochu, C.A., De Celis, A., Codrea, V., Escaso, F., Pérez-García, A. et al. (2020) New diagnosis for *Allodaposuchus precedens*, the type species of the European upper cretaceous clade Allodaposuchidae. *Zoological Journal of the Linnean Society*, 189, 618–634.
- Narváez, I., Brochu, C.A., Escaso, F., Pérez-García, A. & Ortega, F. (2015) New crocodyliforms from southwestern Europe and definition of a diverse clade of European late cretaceous basal eusuchians. *PLoS One*, 10, 1–34.
- Narváez, I., Brochu, C.A., Escaso, F., Pérez-García, A. & Ortega, F. (2016) New Spanish late cretaceous eusuchian reveals the synchronic and sympatric presence of two allodaposuchids. *Cretaceous Research*, 65, 112–125.
- Owen, R. (1842) Report on British fossil reptiles. In: Taylor, R. & Taylor, J.E. (Eds.) *British Association for the Advancement of science for 1841*. London: Owen.
- Owen, R. (1850) On the communications between the cavity of the tympanum and the palate in the Crocodylia (gavials, alligators and crocodiles). *Philosophical Transactions of the Royal Society of London*, 140, 521–527.
- Parrilla-Bel, J., Fortuny, J., Canudo, J.I. & Llacer, S. (2016) Glándulas de la sal en *Maledictosuchus riclaensis* (Metriorhynchidae, Thalattosuchia) del Calloviense de la Península Ibérica. *Geogaceta*, 59, 63–66.
- Pierce, S.E., Williams, M. & Benson, R.B.J. (2017) Virtual reconstruction of the endocranial anatomy of the early Jurassic marine crocodylomorph *Pelegosaurus typus* (Thalattosuchia). *PeerJ*, 5, e3225.
- Platt, S.G., Rainwater, T.R., Thorbjarnarson, J.B. & Martin, D. (2011) Size estimation, morphometrics, sex ratio, sexual size dimorphism, and biomass of *Crocodylus acutus* in the coastal zone of Belize. *Salamandra*, 47, 179–192.
- Pochat-Cottilloux, Y., Martin, J.E., Jouve, S., Perrichon, G., Adrien, J., Salaviale, C. et al. (2022) The neuroanatomy of *Zulmasuchus querejazus* (Crocodylomorpha, Sebectidae) and its implications for the paleoecology of sebecosuchians. *The Anatomical Record*, 305(10), 2708–2728.
- Pol, D., Turner, A.H. & Norell, M.A. (2009) morphology of the late cretaceous crocodylomorph *Shamosuchus djadochtaensis* and a discussion of neosuchian phylogeny as related to the origin of Eusuchia. *Bulletin of the American Museum of Natural History*, 2009(324), 1–103.
- Porter, W.R., Sedlmayr, J.C. & Witmer, L.M. (2016) Vascular patterns in the heads of crocodylians: blood vessels and sites of thermal exchange. *Journal of Anatomy*, 229(6), 800–824.
- Puértolas, E., Canudo, J.I. & Cruzado-Caballero, P. (2011) A new Crocodylian from the late Maastrichtian of Spain: implications for the initial radiation of crocodyloids. *PLoS One*, 6, e20011.
- Puértolas-Pascual, E., Blanco, A., Brochu, C.A. & Canudo, J.I. (2016) Review of the late cretaceous-early Paleogene crocodylomorphs of Europe: extinction patterns across the K-Pg boundary. *Cretaceous Research*, 57, 565–590.
- Puértolas-Pascual, E., Canudo, J.I. & Moreno-Azanza, M. (2014) The eusuchian crocodylomorph *Allodaposuchus subjuniiperus* sp. nov., a new species from the latest cretaceous (upper Maastrichtian) of Spain. *Historical Biology*, 26, 91–109.
- Puértolas-Pascual, E., Serrano-Martínez, A., Pérez-Pueyo, M., Bádenas, B. & Canudo, J.I. (2022) New data on the neuroanatomy of basal eusuchian crocodylomorphs (Allodaposuchidae) from the upper cretaceous of Spain. *Cretaceous Research*, 135, 105170.
- Rio, J.P. & Mannion, P.D. (2021) Phylogenetic analysis of a new morphological dataset elucidates the evolutionary history of Crocodylia and resolves the long-standing gharial problem. *PeerJ*, 9, e12094.
- Rio, J.P., Mannion, P.D., Tschopp, E., Martin, J.E. & Delfino, M. (2020) Reappraisal of the morphology and phylogenetic relationships of the alligatoroid crocodylian *Diplocynodon hantoniensis* from the late Eocene of the United Kingdom. *Zoological Journal of the Linnean Society*, 188, 579–629.
- Ristevski, J. (2022) Neuroanatomy of the mekosuchine crocodylian *Trilophosuchus rackhami* Willis, 1993. *Journal of Anatomy*, 241(4), 981–1013.
- Ristevski, J., Price, G.J., Weisbecker, V. & Salisbury, S.W. (2021) First record of a tomistomine crocodylian from Australia. *Scientific Reports*, 11, 12158.
- Ristevski, J., Yates, A.M., Price, G.J., Molnar, R.E., Weisbecker, V. & Salisbury, S.W. (2020) Australia's prehistoric 'swamp king': revision of the Plio-Pleistocene crocodylian genus *Pallimnarchus* de Vis, 1886. *PeerJ*, 8, e10466.
- Rodrigues, I., de Carvalho, L.B., Azevedo, S.A.K., Maria, F.C. & do Amaral, R.V. (2010) Reconstrução preliminar do ouvido interno de *Mariliasuchus amarali* (Crocodyliformes, Notosuchia) do Neocretáceo do Brasil. *Boletim de Resumos do 7º Simpósio Brasileiro de Paleovertebrados*, 57.
- Salisbury, S.W., Molnar, R.E., Frey, E. & Willis, P.M.A. (2006) The origin of modern crocodyliforms: new evidence from the cretaceous of Australia. *Proceedings of the Royal Society B: Biological Sciences*, 273, 2439–2448.

- Schmidt, K.P. (1928) A new crocodile from New Guinea. *Field Museum of Natural History Publication*, 247(12), 177–181.
- Schmitz, L. (2009) Quantitative estimates of visual performance features in fossil birds. *Journal of Morphology*, 270, 759–773.
- Schwab, J.A., Young, M.T., Herrera, Y., Witmer, L.M., Walsh, S.A., Katsamenis, O.L. et al. (2021) The braincase and inner ear of 'Metriorhynchus' cf. 'M.' *brachyrhynchus* – implications for aquatic sensory adaptations in crocodylomorphs. *Journal of Vertebrate Paleontology*, 41, e1912062.
- Schwab, J.A., Young, M.T., Neenan, J.M., Walsh, S.A., Witmer, L.M., Herrera, Y. et al. (2020) Inner ear sensory system changes as extinct crocodylomorphs transitioned from land to water. *PNAS*, 117, 10422–10428.
- Schwab, J.A., Young, M.T., Walsh, S.A., Witmer, L.M., Herrera, Y., Brochu, C.A. et al. (2022) Ontogenetic variation in the crocodylian vestibular system. *Journal of Anatomy*, 240(5), 821–832.
- Sereno, P.C. & Larsson, H.C.E. (2009) Cretaceous crocodyliforms from the sahara. *ZooKeys*, 28, 1–143.
- Serrano-Martínez, A. (2019) *Análisis de la evolución neurocraneal en la radiación temprana de Eusuchia*. [PhD Thesis]. Spain: UNED, Universidad Nacional de Educación a Distancia.
- Serrano-Martínez, A., Knoll, F., Narváez, I., Lautenschlager, S. & Ortega, F. (2019a) Inner skull cavities of the basal eusuchian *Lohuecosuchus megadontos* (upper cretaceous, Spain) and neurosensorial implications. *Cretaceous Research*, 93, 66–77.
- Serrano-Martínez, A., Knoll, F., Narváez, I., Lautenschlager, S. & Ortega, F. (2021) Neuroanatomical and neurosensorial analysis of the late cretaceous basal eusuchian *Agaresuchus fontisensis* (Cuenca, Spain). *Papers in Palaeontology*, 7, 641–656.
- Serrano-Martínez, A., Knoll, F., Narváez, I. & Ortega, F. (2019b) Brain and pneumatic cavities of the braincase of the basal alligatoroid *Diplocynodon tormis* (Eocene, Spain). *Journal of Vertebrate Paleontology*, 39, e1572612.
- Sertich, J.J.W. & O'Connor, P.M. (2014) A new crocodyliform from the middle cretaceous Galula formation, southwestern Tanzania. *Journal of Vertebrate Paleontology*, 34, 576–596.
- Spix, J.B. (1825) *Animalia nova sive species novae Lacertarum, quas in itinere per Brasiliam annis MDCCCXVII-MDCCCXX jussu et auspiciis Maximiliani Josephi I. Bavaria Regis suscepto collegit et descripsit* D. Munich: J. B. De Pix. Typis Franc. Seraph. Hübschamanni, 26.
- Tarsitano, S.F. (1985) Cranial metamorphosis and the origin of the Eusuchia. *Neues Jahrbuch für Geologie Und Paläontologie Abhandlungen*, 170, 27–44.
- Vergne, A.L., Pritz, M.B. & Mathevon, N. (2009) Acoustic communication in crocodylians: from behaviour to brain. *Biological Reviews*, 84, 391–411.
- Walker, A.D. (1970) A revision of the Jurassic reptile *Hallopus victor* (marsh), with remarks on the classification of crocodiles. *Philosophical Transactions of the Royal Society of London. Series B, Biological Sciences*, 257(816), 323–372.
- Walker, A.D. (1990) A revision of *Sphenosuchus acutus* Haughton, a crocodylomorph reptile from the Elliot formation (late Triassic or early Jurassic) of South Africa. *Philosophical Transactions of the Royal Society of London. Series B, Biological Sciences*, 330, 1–120.
- Walsh, S.A., Barrett, P.M., Milner, A.C., Manley, G.A. & Witmer, L.M. (2009) Inner ear anatomy is a proxy for deducing auditory capability and behaviour in reptiles and birds. *Proceedings of the Royal Society*, 276, 1355–1360.
- Watanabe, A., Gignac, P.M., Balanoff, A.M., Green, T.L., Kley, N.J. & Norell, M.A. (2019) Are endocasts good proxies for brain size and shape in archosaurs throughout ontogeny? *Journal of Anatomy*, 234, 291–305.
- Webb, G.J.W. & Messel, H. (1978) Morphometric analysis of *Crocodylus porosus* from the north coast of Arnhem Land, northern Australia. *Australian Journal of Zoology*, 26, 1–27.
- Whetstone, K.N. & Whybrow, P.J. (1983) A "cursorial" crocodylian from the Triassic of Lesotho (Basutoland), southern Africa. *Occasional Papers of the Museum of Natural History, The University of Kansas*, 106, 1–37.
- Wilberg, E.W., Beyl, A.R., Pierce, S.E. & Turner, A.H. (2022) Cranial and endocranial anatomy of a three-dimensionally preserved teiosaurid thalattosuchian skull. *The Anatomical Record*, 305(10), 2620–2653.
- Witmer, L.M. & Ridgely, R.C. (2008) The paranasal air sinuses of predatory and armored dinosaurs (Archosauria: Theropoda and Ankylosauria) and their contribution to cephalic structure. *The Anatomical Record*, 291, 1362–1388.
- Witmer, L.M. & Ridgely, R.C. (2009) New insights into the brain, braincase, and ear region of tyrannosaurs (Dinosauria, Theropoda), with implications for sensory organization and behavior. *The Anatomical Record*, 292, 1266–1296.
- Witmer, L.M., Ridgely, R.C., Dufeu, D.L. & Semones, M.C. (2008) Using CT to peer into the past: 3D visualization of the brain and ear regions of birds, crocodiles, and nonavian dinosaurs. *Anatomical Imaging*, 67–87.
- Yeh, H.K. (1958) A new crocodile from Maoming, Kwangtung. *Vertebrata Palasiatica*, 2, 237–242.
- Zelenitsky, D.K., Therrien, F. & Kobayashi, Y. (2009) Olfactory acuity in theropods: palaeobiological and evolutionary implications. *Proceedings of the Royal Society B: Biological Sciences*, 276, 667–673.
- Zelenitsky, D.K., Therrien, F., Ridgely, R.C., McGee, A.R. & Witmer, L.M. (2011) Evolution of olfaction in non-avian theropod dinosaurs and birds. *Proceedings of the Royal Society B: Biological Sciences*, 278, 3625–3634.

SUPPORTING INFORMATION

Additional supporting information can be found online in the Supporting Information section at the end of this article.

How to cite this article: Puértolas-Pascual, E., Kuzmin, I.T., Serrano-Martínez, A. & Mateus, O. (2023) Neuroanatomy of the crocodylomorph *Portugalosuchus azenhae* from the late cretaceous of Portugal. *Journal of Anatomy*, 00, 1–26.
Available from: <https://doi.org/10.1111/joa.13836>